International Journal of Future Engineering Innovations

Phosphorus Control in Titanium Feedstocks for Tio₂ Pigment Production: A Critical Review of Mineralogical Constraints, Dephosphorization Routes, and Rutilization Performance

Antonio Clareti Pereira
PhD, Department of Graduate Program in Materials Engineering, Federal University of Ouro Preto (UFOP), Ouro Preto, MG, Brazil

Corresponding Author: **Antonio Clareti Pereira**

Article Info

ISSN (online): 3049-1215
Impact Factor (RSIF): 8.25
Volume: 03
Issue: 02
March-April 2026
Received: 23-12-2025
Accepted: 25-01-2026
Published: 27-02-2026
Page No: 08-30

Abstract
Phosphorus control in titanium feedstocks is a critical yet often underestimated requirement for producing pigment-grade TiO_2. Across primary ores, upgraded feedstocks, and industrial processing routes, residual phosphorus—commonly reported as P or P_2O_5—emerges as a key risk factor that governs calcination behavior, rutilization efficiency, and ultimately pigment commercial viability. This critical review examines the mineralogical occurrence and deportment of phosphorus in titanium ores and Ti-bearing feedstocks. It systematically evaluates physical beneficiation, hydrometallurgical, and pyrometallurgical dephosphorization strategies from processing and performance perspectives. Particular emphasis is placed on mineralogical constraints on phosphorus removal, including limitations on liberation, microscale textural associations, and phosphorus redistribution during upgrading. Beyond removal efficiency metrics, the review highlights that P_2O_5 directly suppresses the anatase-to-rutile transformation during calcination by segregating at grain boundaries and stabilizing anatase, yielding mixed-phase pigments that are non-commercial despite high TiO_2 grades. Comparative analysis shows that physical beneficiation alone rarely meets phosphorus thresholds compatible with reliable rutilization; hydrometallurgical routes offer higher selectivity but introduce trade-offs in titanium recovery and effluent management; and pyrometallurgical upgrading to Ti-rich slags enables indirect phosphorus control through elemental partitioning when slag chemistry is explicitly engineered. The review concludes that robust phosphorus control requires integrated, feedstock-specific dephosphorization strategies optimized against rutilization performance rather than bulk chemical specifications, reframing feedstock qualification as a pigment-oriented engineering challenge.

DOI: https://doi.org/10.54660/IJFEI.2026.3.2.08-30

Keywords: Titanium ores, Phosphorus removal, P_2O_5, TiO_2 pigment, Rutile formation, Calcination

1. Introduction

Titanium dioxide (TiO_2) feedstock upgrading remains a central challenge for the pigment industry, with performance and marketability tightly coupled to impurity control and downstream process compatibility. Natural and upgraded titanium resources—including ilmenite, rutile, anatase ores, synthetic rutile, and Ti-bearing slags—exhibit wide variability in gangue assemblages and trace-element burdens, which strongly influence beneficiation response and extractive flowsheet selection (Thambiliyagodage *et al*., 2021; Subasinghe & Ratnayake, 2023; Tahooni Bonab *et al*., 2025) [54, 51, 53]. From a mineral processing perspective, ilmenite flotation and related surface-chemistry controls have been extensively reviewed, highlighting collector adsorption mechanisms, surface dissolution effects, and the dependence of separation efficiency on mineralogical liberation and textural constraints (Zhai *et al*., 2020; Fang *et al*., 2020; Zhang, H. *et al*., 2022) [67, 10, 69].

In parallel, hydrometallurgical routes—such as direct acid leaching in HCl/H_2SO_4 and variants enabled by pre-treatments—have been developed for low-grade or complex feeds, with kinetics, leaching chemistry, and downstream separation issues increasingly well documented (Anggraeni *et al*., 2023; Ahn & Lee, 2021; Dubenko *et al*., 2020; Rotich *et al*., 2024; Long *et al*., 2025) [4, 1, 9, 46, 26].

In this upgrading landscape, phosphorus (typically reported as P or P_2O_5) is a particularly problematic impurity because it is commonly associated with phosphate minerals (e.g., apatite) and Fe–Ti–P ore systems, and may be disseminated at fine scales that hinder removal by conventional physical separations. Geological and mineralogical studies consistently show that apatite and phosphate phases co-occur with Fe–Ti oxides across multiple deposit types, indicating that phosphorus deportment is often structurally inherent to the ore rather than a superficial contaminant (Reich *et al*., 2022; Nabil & Barnes, 2022; Miloski *et al*., 2024; Kepezhinskas *et al*., 2024) [44, 37, 34, 18]. This association underscores the importance of rigorous mineralogical characterization and liberation analysis prior to process selection, particularly when phosphate occurs as inclusions or intergrowths with Fe–Ti oxides—features that frequently limit attainable separation selectivity and recovery (Alfonso *et al*., 2020; Üçerler-Çamur *et al*., 2025; Yang *et al*., 2021) [2, 56, 63].

From an industrial standpoint, the primary concern is not merely the presence of phosphorus in the feed but its functional impact on pigment manufacturing. Residual P_2O_5 is widely regarded as a critical "killer impurity" because it compromises the formation of pigment-grade rutile during calcination, yielding mixed-phase rutile–commercially unacceptable anatase products. Despite its practical importance, the literature remains fragmented regarding quantitative thresholds and robust links among P_2O_5 levels, calcination conditions, and rutilization outcomes, underscoring the need for a dedicated, pigment-oriented critical assessment.

Technologically, phosphorus control spans three main intervention domains: (i) mineral processing routes targeting phosphate deportment, including flotation-based removal demonstrated in complex phosphorus-bearing systems; (ii) hydrometallurgical routes in which roasting or activation enables selective dissolution; and (iii) thermochemical or slag-based strategies that partition phosphorus away from TiO_2-rich products (Xiao *et al*., 2020; De Oliveira *et al*., 2023; Chen *et al*., 2024; Qu *et al*., 2024) [61, 8, 6, 42]. The effectiveness of these approaches is constrained by ore mineralogy, liberation degree, and the tendency of intensified treatments to shift impurities into solution phases that require further purification, thereby increasing reagent and effluent burdens (Azamat *et al*., 2021; Pysarenko *et al*., 2023; Stopic *et al*., 2024) [5, 41, 49]. Moreover, reliable phosphorus determination in high-titanium matrices remains analytically challenging and may bias reported removal efficiencies if not carefully controlled (Mogashane *et al*., 2025) [36].

This review critically examines phosphorus occurrence, deportment, and removal strategies in titanium ores and Ti-bearing feedstocks, explicitly framed by pigment-grade TiO_2 production requirements and the industrial risk posed by residual P_2O_5 during calcination. Evidence from physical beneficiation, hydrometallurgical dephosphorization, and thermochemical/slag-based routes is synthesized, with emphasis on (a) mineralogical controls and liberation constraints, (b) phosphorus removal efficiency versus titanium losses and process penalties, (c) compatibility with downstream pigment processing, and (d) research gaps that limit transferable process-selection criteria.

To ensure transparency and reproducibility consistent with Minerals Engineering standards, the next section details the methodology for compiling and evaluating the literature, including database selection, keyword logic, screening workflow, and the criteria used to compare studies consistently.

Graphical abstract

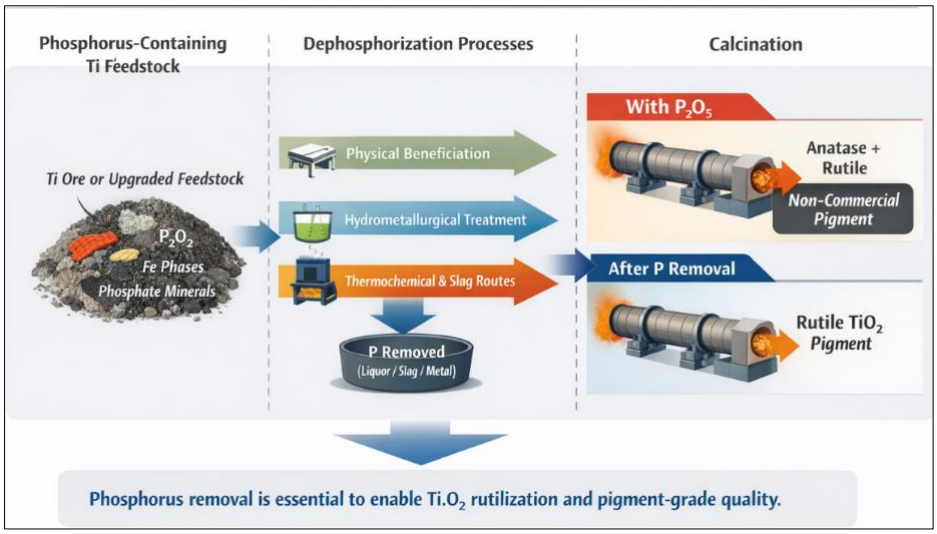

Fig 1:

2. Methodology

This critical review was conducted in accordance with the PRISMA 2020 reporting principles, adapted for a structured yet non-systematic review framework suitable for mineral processing and extractive metallurgy studies (Page *et al*., 2021) [39]. The objective was to critically assess phosphorus

occurrence, deportment, and removal strategies in titanium ores and Ti-bearing feedstocks, with explicit emphasis on pigment-grade TiO_2 production and calcination behavior.

A comprehensive literature search was conducted using Scopus, Web of Science, ScienceDirect, and Google Scholar, covering peer-reviewed articles, reviews, theses, and selected conference proceedings. Search strings combined terms for titanium resources and processing (e.g., ilmenite, rutile, titanium slag, TiO_2 feedstocks), phosphorus (P, P_2O_5, phosphate, apatite), and pigment-relevant process stages (beneficiation, leaching, dephosphorization, calcination, anatase–rutile transformation). Priority was given to publications from 2020–2025, with earlier seminal studies included where mechanistically relevant.

Studies were screened for relevance to titanium feedstocks, explicit treatment or quantification of phosphorus, applicability to physical, hydrometallurgical, or thermochemical routes, and implications for downstream pigment production. Publications unrelated to mineral feedstocks or pigment-oriented processing were excluded unless they provided transferable mechanistic insights. After screening and consolidation, 72 references were retained and constitute the bibliographic basis of this review.

Data extraction focused on feed mineralogy, phosphorus form and analytical determination, removal efficiency, titanium losses, process conditions, and reported links to calcination behavior. The literature was synthesized thematically—rather than statistically—into physical beneficiation, hydrometallurgical, and thermochemical approaches, with comparative emphasis on process–structure–property relationships and the role of phosphorus control in enabling complete rutilization.

Figure 1 summarizes the PRISMA 2020–based screening and selection workflow used in this review, including database identification, exclusion criteria, and the final inclusion of studies relevant to phosphorus control in titanium feedstocks.

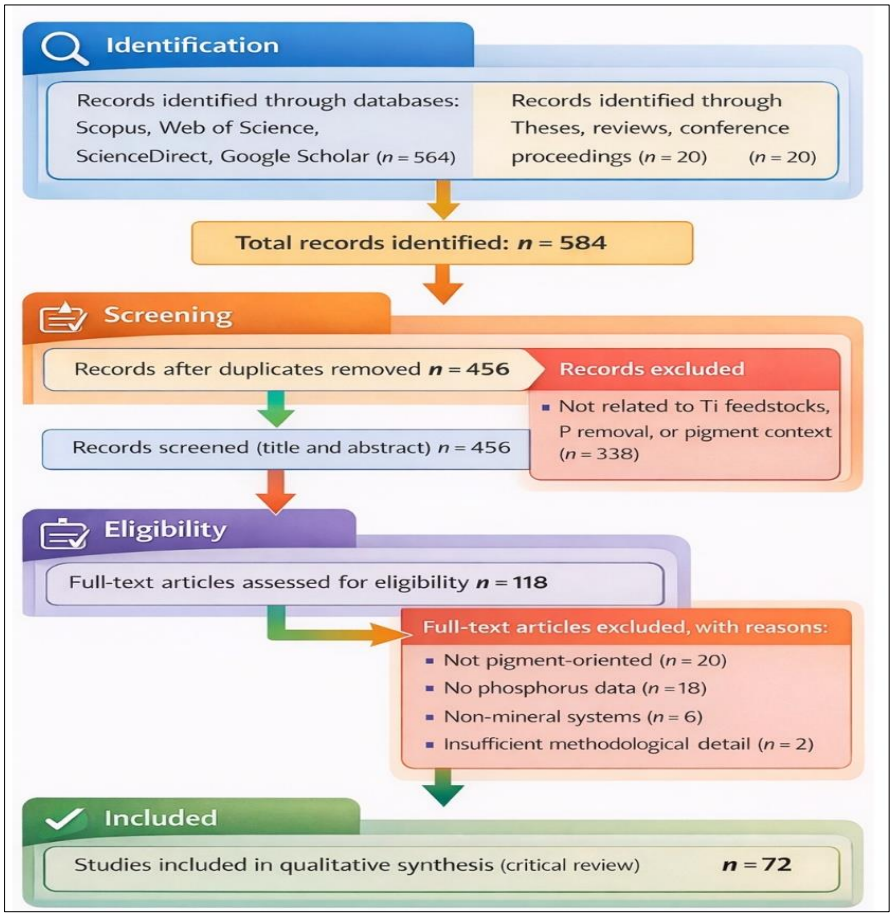

Fig 2: The PRISMA 2020 flow diagram summarizing the literature identification, screening, eligibility, and inclusion steps. Adapted from: Page *et al*. (2021).

As shown in Figure 1, most excluded studies were removed during the screening and eligibility stages due to lack of relevance to pigment-oriented titanium processing, the absence of phosphorus data, or a focus on non-mineral systems. Only studies with sufficient methodological detail and explicit relevance to phosphorus deportment, removal strategies, and downstream implications for TiO_2 pigment production were retained in the final qualitative synthesis.

3. Occurrence and mineralogical controls of phosphorus in titanium ores and feedstocks

The occurrence and distribution of phosphorus in titanium ores are primarily governed by ore genesis, mineralogical assemblage, and post-depositional alteration. Across magmatic, magmatic–hydrothermal, and sedimentary environments, phosphorus is predominantly hosted in phosphate minerals—mainly apatite—commonly associated with Fe–Ti oxides such as ilmenite, titanomagnetite, and magnetite (Reich *et al*., 2022; Nabil & Barnes, 2022) [44, 37]. Detailed mineralogical studies show that apatite occurs as discrete grains, micro-inclusions, or complex intergrowths formed during magmatic crystallization or hydrothermal remobilization, directly controlling phosphorus liberation during processing (Miloski *et al*., 2024; Kepezhinskas *et al*.,

2024; Zeng *et al*., 2022) [34, 18, 66].

Investigations of titaniferous iron ores and ilmenite-rich deposits further demonstrate that phosphorus distribution is highly heterogeneous at the grain scale. Phosphate phases are often finely disseminated or encapsulated within Fe–Ti oxides, a texture that severely limits conventional physical separation (Khedr *et al*., 2024; Mandende & Mothupi, 2024) [19, 31]. Quantitative mineralogical techniques such as MLA and QEMSCAN reveal that low bulk phosphorus levels may still reflect persistent phosphorus-rich microdomains, underscoring the limitations of bulk chemical assays without mineralogical context (Üçerler-Çamur *et al*., 2025; Yang *et al*., 2021; Wulan *et al*., 2021) [56, 63, 59].

From a processing perspective, the mineralogical form of phosphorus governs both its removability and downstream behavior. When phosphorus is hosted in apatite-rich domains, flotation-based approaches may achieve partial removal, as demonstrated in phosphorus-bearing vanadium–titanium magnetite tailings (Xiao *et al*., 2020) [61]. In contrast, when phosphorus is structurally bound within Fe–Ti oxides or present as ultra-fine inclusions, liberation constraints dominate, and physical methods rapidly reach their practical limits (Zhai *et al*., 2020; Fang *et al*., 2020) [67, 10] consistent with broader observations that liberation controls separation efficiency in complex oxide systems (Alfonso *et al*., 2020; Lv
et al., 2020) [2, 28].

Upgraded titanium feedstocks—including synthetic rutile, titanium slags, and leaching residues—introduce additional complexity. Thermochemical treatments may redistribute phosphorus among solid phases, slags, and metallic products, potentially concentrating it in TiO_2-rich residues if poorly controlled (Qu *et al*., 2024; Subasinghe & Ratnayake, 2023) [42, 51]. Hydrometallurgical routes, especially alkaline roasting and acid leaching, further modify phosphorus speciation by transferring it into solution phases that require subsequent purification (De Oliveira *et al*., 2023; Chen *et al*., 2024; Pysarenko *et al*., 2023) [8, 6, 41]. Cross-study comparisons are further complicated by inconsistencies in phosphorus analysis for high-titanium matrices, which may bias reported removal efficiencies (Mogashane *et al*., 2025) [36].

Beyond process efficiency, phosphorus occurrence has direct implications for pigment production. Phosphorus retained in Ti-bearing solids—either as residual phosphates or structurally incorporated species—can persist in TiO_2 precursors and influence phase evolution during calcination. Accordingly, a mineralogical scale understanding of phosphorus occurrence is essential for interpreting its impact on TiO_2 crystallization and pigment quality, rather than treating phosphorus solely as a bulk impurity.

The mineralogical mode of phosphorus occurrence exerts a first-order control on its behavior during processing and on the effectiveness of downstream dephosphorization strategies. To synthesize the key mineralogical patterns reported for titanium ores and feedstocks, Table 1 summarizes the principal phosphorus host phases, textural associations, and their implications for liberation and physical removal.

Table 1: Mineralogical modes of phosphorus occurrence in titanium ores and feedstocks. Adapted from: Reich *et al*. (2022); Nabil and Barnes (2022); Alfonso *et al*. (2020); Xiao *et al*. (2020); Zhai *et al*. (2020); Subasinghe and Ratnayake (2023) [51]; Miloski *et al*. (2024); Kepezhinskas *et al*. (2024); Üçerler-Çamur *et al*. (2025).

Ore / feedstock type	Host mineral(s) of phosphorus	Typical textural association	Implications for liberation	Expected amenability to physical removal
Magmatic ilmenite ores	Apatite	Discrete grains; coarse intergrowths with Fe–Ti oxides	Moderate to good liberation at medium grind sizes	Moderate; gravity and flotation may be effective
Vanadium–titanium magnetite ores	Apatite; minor solid solution in oxides	Fine inclusions within magnetite and ilmenite	Poor liberation; encapsulation dominates	Low; physical routes rapidly reach limits
Magmatic–hydrothermal Fe–Ti deposits	Apatite; secondary phosphates	Complex intergrowths; remobilized veinlets	Variable liberation depending on alteration intensity	Low to moderate; selective flotation sometimes viable
Sedimentary and placer ilmenite	Apatite; detrital phosphates	Discrete liberated grains	Good liberation at coarse sizes	High; gravity and magnetic separation effective
Synthetic rutile	Residual apatite; structurally incorporated P	Ultra-fine inclusions; lattice-bound species	Very limited liberation	Very low; physical removal ineffective
Titanium slags (high-Ti)	Phosphate-rich slag phases	Amorphous or glassy slag domains	Liberation not applicable	Not applicable; requires thermochemical control
Leaching residues	Secondary phosphates	Fine precipitates coating TiO_2 particles	Poor liberation; surface-bound phases	Low; chemical re-treatment required

As shown in Table 1, the effectiveness of physical dephosphorization methods is strongly constrained by the mineralogical form and texture of phosphorus-bearing phases. While discrete apatite grains in placer or weakly altered ores may be amenable to gravity or flotation-based removal, phosphorus occurring as fine inclusions or structurally bound species in Fe–Ti oxides and upgraded feedstocks severely limits the applicability of physical beneficiation alone. These mineralogical constraints motivate the integration of hydrometallurgical or thermochemical strategies into pigment-oriented flowsheets.

The mineralogical mode of phosphorus occurrence in Fe–Ti oxide systems decisively influences liberation behavior and, consequently, the effectiveness of physical dephosphorization methods. To illustrate how different textural associations, govern phosphorus deportment and separation potential, Figure 2 presents a schematic comparison of liberated apatite grains with apatite occurring as inclusions within Fe–Ti oxides.

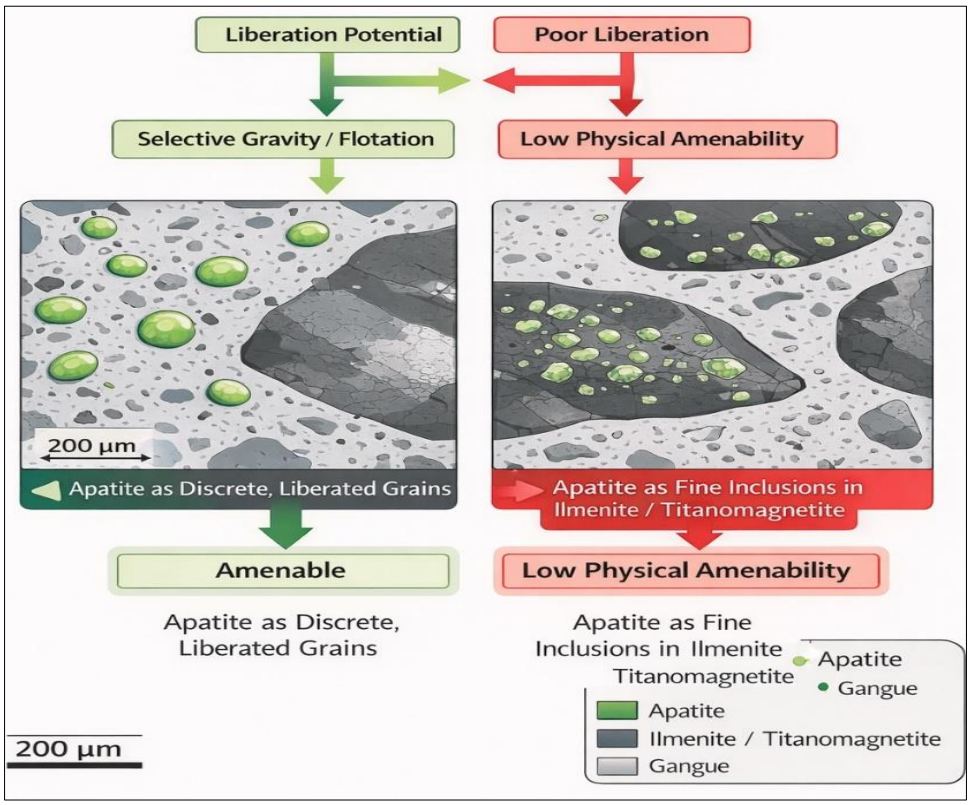

Fig 3: Schematic illustration of phosphorus deportment in Fe–Ti oxide systems, apatite as discrete grains. Adapted from: Alfonso *et al*. (2020); Zhai *et al*. (2020); Xiao *et al*. (2020); Reich *et al*. (2022); Miloski *et al*. (2024); Kepezhinskas *et al*. (2024).

As illustrated in Figure 2, apatite, when present as discrete, liberated grains, can be selectively removed by gravity concentration or flotation, provided adequate liberation is achieved. In contrast, apatite occurring as fine inclusions or intergrowths within ilmenite or titanomagnetite shows poor liberation, sharply limiting the effectiveness of physical beneficiation. These mineralogical constraints explain why physical methods alone are often insufficient for phosphorus control in complex Fe–Ti oxide systems and justify integrating hydrometallurgical or thermochemical dephosphorization strategies into pigment-oriented processing flowsheets.

The mineralogical analysis presented in Section 3 shows that the occurrence and deportment of phosphorus in titanium ores are fundamentally governed by ore type, textural relationships, and upgrading history. However, mineralogical control alone does not determine process viability for pigment manufacture. The industrial relevance of phosphorus contamination ultimately depends on the type of titanium feedstock entering the pigment production route and on the chemical and phase-purity requirements imposed by sulfate- and chloride-based processes. Accordingly, Section 4 reviews the primary and secondary titanium feedstocks used for TiO_2 pigment production, their typical impurity profiles, and the feedstock-specific phosphorus constraints that frame the severity of the phosphorus problem discussed in subsequent sections.

4. Titanium ores and feedstocks for pigment production

4.1. Primary titanium ores

Primary titanium ores form the basis of most pigment production routes and include ilmenite, rutile, anatase, and leucoxene. Ilmenite ($FeTiO_3$) is the most abundant and widely exploited titanium mineral, serving as the principal feedstock for sulfate-route digestion and for upgrading processes that yield higher-grade intermediates (Zhai *et al*., 2020; Thambiliyagodage *et al*., 2021) [67, 54]. Natural rutile, composed mainly of TiO_2, is the most chemically suitable feedstock because of its high titanium content and low impurity levels; however, its limited availability necessitates continued reliance on ilmenite-derived materials (Xu & Wang, 2025; Tahooni Bonab *et al*., 2025) [62, 53].

Anatase and leucoxene occur as primary phases or as alteration products of ilmenite and titanomagnetite. Although anatase-rich ores may have high TiO_2 contents, associations with iron, phosphorus, and silicate phases often limit their direct use in pigment production (De Oliveira *et al*., 2023; Dubenko *et al*., 2020) [8, 9]. Leucoxene, formed by weathering and oxidation of ilmenite, typically has elevated TiO_2 but retains residual gangue and trace elements inherited from the parent mineral, including phosphorus associated with remnant apatite or Fe–Ti–P microdomains (Mandende & Mothupi, 2024; Khedr *et al*., 2024) [31, 19]. Consequently, even apparently high-grade primary ores often require further upgrading to meet pigment feedstock specifications.

Primary titanium ores show substantial variability in TiO_2 grade and impurity profiles, which directly affect their suitability for pigment production routes and the intensity of required upgrading steps. Table 2 summarizes the typical TiO_2 contents, major impurity levels, and key processing implications for the main primary titanium ores used by the pigment industry.

Table 2: Primary titanium ores used for pigment production: typical TiO_2 content, major impurities, and processing implications. Adapted from: Zhai *et al*. (2020); Thambiliyagodage *et al*. (2021); Dubenko *et al*. (2020); Mandende & Mothupi (2024); Khedr *et al*. (2024); Xu & Wang (2025); Tahooni Bonab *et al*. (2025).

Ore type	Typical TiO_2 content (wt%)	Major impurities	Processing implications for pigment production
Ilmenite ($FeTiO_3$)	45–55	FeO/Fe_2O_3 (30–40%), P_2O_5 (0.05–0.5%), V_2O_5 (0.1–0.4%)	Requires digestion (sulfate route) or upgrading to synthetic rutile or Ti-rich slag; phosphorus control critical to avoid calcination issues
Rutile (natural)	90–96	Fe_2O_3 (<1%), P_2O_5 (<0.02%), V_2O_5 (<0.1%)	Ideal feedstock for chloride route; limited availability restricts large-scale reliance
Anatase-rich ores	70–85	Fe_2O_3 (1–5%), P_2O_5 (0.05–0.3%), SiO_2 (variable)	High TiO_2 but impurity associations may hinder direct pigment use; sensitive to P_2O_5-induced rutilization inhibition
Leucoxene	80–90	Residual Fe oxides, P_2O_5 (0.05–0.4%), SiO_2	Often requires beneficiation or chemical upgrading; residual phosphorus linked to parent ilmenite texture
Titaniferous magnetite	10–25 (bulk ore)	Fe oxides (dominant), P_2O_5 (0.1–0.6%), V_2O_5	Not a direct pigment feedstock; requires concentration and upgrading to Ti-rich intermediates

As shown in Table 2, even ores with relatively high TiO_2 content may fail to meet pigment feedstock requirements because of elevated levels of iron, phosphorus, or vanadium. Among these impurities, P_2O_5 is particularly critical because even small residual concentrations can adversely affect downstream calcination and rutile formation. Consequently, impurity management—especially phosphorus control- often governs the selection of upgrading routes and determines whether a given ore can be economically integrated into sulfate- or chloride-based pigment production flowsheets.

4.2. Secondary and upgraded titanium feedstocks

To address the limited availability of natural rutile, industrial pigment production relies on secondary and upgraded feedstocks, notably synthetic rutile, titanium slags, and upgraded ilmenites. Synthetic rutile is typically produced by selective iron removal from ilmenite via reductive roasting followed by leaching or related upgrading routes, yielding a TiO_2-rich solid suitable for chloride processing (Subasinghe & Ratnayake, 2023 [51]; Spencer *et al*., 2025) [51, 48]. However, phosphorus initially present in the ilmenite may be redistributed during upgrading and persist in the final product if not specifically controlled.

Titanium slags produced by ilmenite smelting constitute another primary feedstock, particularly for chloride-route pigment production. These slags generally contain 70–90 wt% TiO_2 and benefit from simultaneous iron removal; nevertheless, phosphorus partitioning during smelting depends strongly on slag chemistry and operating conditions, and incomplete rejection may leave residual P_2O_5 levels problematic for downstream processing (Qu *et al*., 2024; Subasinghe & Ratnayake, 2023) [42, 51].

Secondary titanium feedstocks are produced through a sequence of upgrading steps that increase TiO_2 content and remove iron from ilmenite. However, these transformations may also redistribute phosphorus among solid, liquid, and slag phases, with important implications for downstream pigment processing. Figure 3 schematically summarizes the main industrial upgrading pathways from ilmenite to synthetic rutile and to TiO_2-rich slags, highlighting the stages at which phosphorus may persist or re-concentrate.

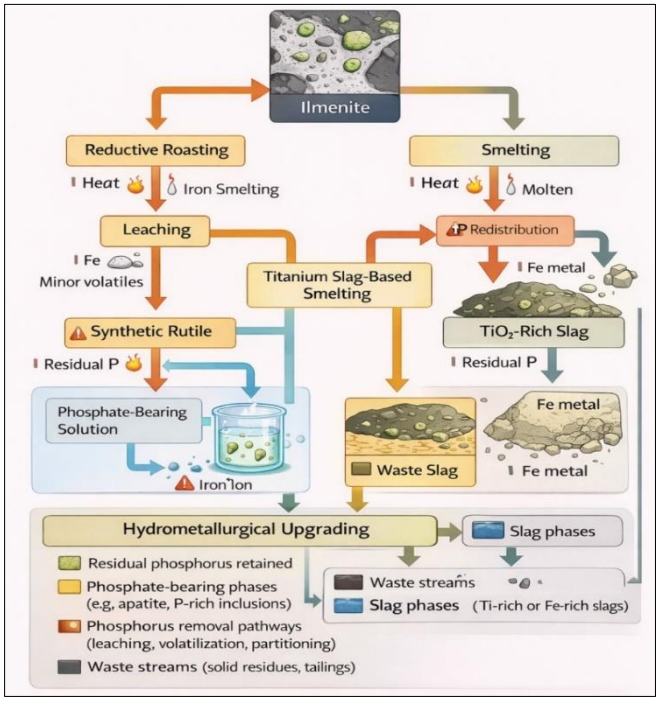

Fig 4 : Simplified upgrading pathways from ilmenite to secondary titanium feedstocks, including synthetic rutile and TiO_2-rich slags. Adapted from: Subasinghe and Ratnayake (2023) [51]; Qu *et al*. (2024); Chen *et al*. (2024); Pysarenko *et al*. (2023); Spencer *et al*. (2025).

As shown in Figure 3, upgrading routes that effectively remove iron do not necessarily ensure proportional phosphorus rejection. In synthetic rutile production, phosphorus may remain associated with TiO_2-rich solids after reductive roasting and leaching, whereas smelting-based routes may transfer phosphorus to slag or metal phases depending on slag chemistry and operating conditions. Subsequent hydrometallurgical treatments can further modify phosphorus speciation, often shifting it into solution streams that require additional purification. These redistribution pathways explain why upgraded feedstocks with high TiO_2 grades may still pose phosphorus-related challenges during calcination and pigment production.

Subsequent hydrometallurgical upgrading can further modify phosphorus speciation, transferring it to solid residues or leach solutions that require additional purification (Chen *et al*., 2024; Pysarenko *et al*., 2023) [6, 41].

Overall, the variability in phosphorus behavior across upgraded feedstocks highlights a key limitation in the literature: classification is often based solely on TiO_2 grade, while residual impurity chemistry—particularly phosphorus—is underreported or inconsistently quantified, hindering meaningful comparisons across studies and industrial routes (Mogashane *et al*., 2025) [36].

Table 3 shows that upgrading routes designed to increase TiO_2 content do not inherently ensure effective phosphorus removal. Residual or redistributed phosphorus may persist in high-grade feedstocks, underscoring the need for explicit dephosphorization strategies aligned with calcination performance and pigment quality requirements.

Table 3: Secondary and upgraded titanium feedstocks for pigment production: TiO_2 grade, phosphorus behavior, and processing implications. Adapted from: Subasinghe and Ratnayake (2023) [51]; Qu *et al*. (2024); Chen, *et al*. (2024); Pysarenko *et al*. (2023); Spencer *et al*. (2025); Mogashane *et al*. (2025)

Feedstock	Typical TiO_2 content (wt%)	Main upgrading route	Typical phosphorus behavior	Implications for pigment production
Synthetic rutile	88–95	Reductive roasting + leaching (or variants)	P may remain with TiO_2-rich solids if not explicitly targeted	High TiO_2 suitable for chloride route; residual P_2O_5 can inhibit rutilization during calcination
TiO_2-rich slag	70–90	Smelting of ilmenite concentrates	P partitioning depends on slag chemistry and operating conditions; incomplete rejection possible	Effective Fe removal; residual P_2O_5 may persist and affect downstream processing
Upgraded ilmenite	60–75	Physical beneficiation + thermal/chemical upgrading	Partial redistribution of P; speciation altered by treatment	Intermediate feedstock; often requires further dephosphorization for pigment use
Leaching residues (Ti-rich)	75–95 (solid residue)	Acid or alkaline leaching	P transferred to solids or solutions, requiring additional purification	High Ti grades achievable; impurity control governs pigment suitability

4.3. Pigment production routes and feedstock purity requirements

The sulfate and chloride routes dominate industrial TiO_2 pigment production, each imposing distinct constraint on feedstock chemistry. The sulfate process is more tolerant of impurities and can process lower-grade ilmenites and leucoxenes; however, elevated phosphorus levels interfere with digestion, hydrolysis, and waste management, causing operational inefficiencies and product-quality penalties (Thambiliyagodage *et al*., 2021; Tahooni Bonab *et al*., 2025) [54, 53]. In contrast, the chloride process requires high-purity feedstocks—natural or synthetic rutile and TiO_2-rich slags—with strict limits on deleterious elements, including phosphorus, to prevent reactor fouling, undesirable by-products, and pigment defects (Qu *et al*., 2024; Xu & Wang, 2025) [42, 62].

For both routes, acceptable phosphorus levels are ultimately governed by calcination performance, because residual P_2O_5 in TiO_2 precursors can impair phase transformation and pigment quality regardless of upstream processing. Nevertheless, feedstock specifications often report phosphorus only as bulk chemical data, without linking it to rutilization behavior or pigment performance. This gap underscores the need to frame phosphorus control as a pigment-oriented design criterion rather than a secondary chemical specification.

Table 4 shows that although the sulfate route offers greater flexibility in feedstock chemistry, phosphorus remains a critical impurity because of its effects on digestion, hydrolysis, and calcination. In the chloride route, phosphorus tolerance is significantly lower, and residual P_2O_5 directly compromises chlorination stability and rutilization performance, thereby defining feedstock acceptability. Across both routes, phosphorus control is a pigment-oriented constraint rather than a purely chemical specification.

Table 4: Comparison of sulfate and chloride pigment routes: feedstock requirements, impurity tolerance, and critical phosphorus constraints. Adapted from: Thambiliyagodage *et al*. (2021); Tahooni Bonab *et al*. (2025); Qu *et al*. (2024); Xu & Wang (2025).

Aspect	Sulfate process	Chloride process
Typical feedstocks	Ilmenite, leucoxene, upgraded ilmenite	Natural rutile, synthetic rutile, TiO_2-rich slags
Typical TiO_2 content of feedstock (wt%)	45–65 (ilmenite), up to ~80 (leucoxene/upgraded feeds)	≥90 (rutile/synthetic rutile), 70–90 (slag)
Tolerance to impurities	Relatively high	Very low
Key deleterious impurities	P_2O_5, Fe, MgO, CaO, alkalis	P_2O_5, V, Cr, Fe, alkalis
Typical phosphorus limits	Moderate; depends on digestion and waste control	Very strict; dictated by chlorination and calcination behavior
Impact of phosphorus in upstream processing	Interference in digestion and hydrolysis; increased waste complexity	Reactor fouling, by-product formation during chlorination
Impact of phosphorus on calcination	Inhibits complete rutilization; promotes mixed anatase–rutile pigments	Strong inhibition of rutilization; severe pigment quality loss
Flexibility in feedstock selection	High	Low
Typical industrial response to high P_2O_5	Blending, partial dephosphorization, waste dilution	Feedstock rejection or dedicated dephosphorization
Strategic implication for P control	Operational optimization	Feedstock gatekeeper criterion

Section 4 establishes that titanium ores and upgraded feedstocks exhibit wide variability in phosphorus content and deportment, and that pigment production routes impose increasingly stringent constraints on feedstock purity. However, these specifications alone do not fully explain why phosphorus is considered one of the most critical impurities in TiO_2 manufacturing. The decisive impact of phosphorus emerges during calcination, when residual P_2O_5 directly affects TiO_2 phase evolution and pigment performance. Accordingly, Section 5 examines phosphorus's impact on TiO_2 pigment quality, with particular emphasis on its inhibitory role in the anatase-to-rutile transformation and the resulting loss of commercial value.

5. Impact of phosphorus on TiO_2 pigment quality

5.1. Chemical and processing impacts of phosphorus

Phosphorus exerts a multifaceted influence on TiO_2 pigment manufacturing, affecting final phase composition and upstream chemical operations in sulfate and chloride routes. During acid digestion and hydrolysis, phosphorus-bearing species may dissolve and reprecipitate as phosphate complexes, altering solution chemistry and narrowing process control windows (Tahooni Bonab *et al*., 2025; Thambiliyagodage *et al*., 2021) [53, 54]. In sulfate-route processing, elevated phosphorus has been linked to secondary-phase formation and unstable hydrolysis behavior, complicating particle-size control and filtration (Anggraeni *et al*., 2023; Dubenko *et al*., 2020) [4, 9].

Chemically, phosphate ions readily interact with Ti(IV) species, forming titanium–phosphate complexes or mixed oxyphosphate phases that may persist through precipitation and calcination unless effectively removed. Studies of titanium phosphates and phosphorus-modified TiO_2 highlight strong Ti–O–P bonding and altered thermal stability relative to pure TiO_2. While these effects are exploited in functional materials, they are detrimental to pigment manufacturing, where phase purity and controlled crystallization are critical. Phosphorus further affects impurity recycling loops and waste streams, accumulating in recycled liquors or solid residues and increasing waste-treatment complexity in both sulfate and chloride processes (Chen *et al*., 2024; De Oliveira *et al*., 2023) [6, 8]. Inconsistent reporting of phosphorus speciation and incomplete mass balances often obscure its circulation within pigment plants, leading to underestimation of long-term operational impacts (Mogashane *et al*., 2025) [36]. Overall, these effects confirm that phosphorus is an active participant in TiO_2 processing chemistry rather than a passive impurity.

Table 5 shows that phosphorus affects TiO_2 pigment manufacturing at multiple stages, from solution chemistry during digestion and hydrolysis to impurity buildup in recycle streams. These effects indicate that phosphorus

Table 5 : Chemical and process-level impacts of phosphorus in TiO_2 pigment production and reported consequences. Adapted from: Thambiliyagodage *et al*. (2021); Dubenko *et al*. (2020); Anggraeni *et al*. (2023); Tahooni Bonab *et al*. (2025); Chen *et al*. (2024); De Oliveira *et al*. (2023); Mogashane *et al*. (2025).

Process stage	Form of phosphorus involved	Main chemical/process interaction	Reported operational impact	Implications for pigment quality
Acid digestion (sulfate route)	Dissolved phosphate species, apatite-derived P	Partial dissolution and reprecipitation as phosphate complexes; altered liquor chemistry	Narrowed operating window; reduced digestion efficiency	Indirect impact via unstable downstream hydrolysis
Hydrolysis	Ti–phosphate complexes; mixed oxyphosphate species	Interference with Ti(IV) hydrolysis and nucleation	Poor particle size control; filtration difficulties	Broader PSD; reduced pigment consistency
Precipitation / solid intermediates	Structurally incorporated P; Ti–O–P bonds	Stabilization of non-ideal precursor phases	Persistence of P into calcination feed	Incomplete rutilization
Calcination (indirect effect)	Residual P_2O_5 in TiO_2 precursors	Inhibition of anatase–rutile transformation	Mixed anatase–rutile products	Non-commercial pigment
Recycle liquors	Dissolved phosphate species	Accumulation in closed-loop systems	Increased impurity build-up; complex bleed management	Long-term process instability
Solid residues / wastes	Phosphate-rich solids	Concentration of P in residues and sludges	More complex waste treatment and disposal	No direct benefit; regulatory burden

5.2. Inhibition of TiO_2 rutile formation by P_2O_5 during calcination

The most severe consequence of phosphorus contamination occurs during the calcination stage, where the anatase-to-rutile transformation must proceed to completion to yield pigment-grade TiO_2. This transformation is a reconstructive phase change that requires atomic diffusion, lattice rearrangement, and controlled crystal growth. Residual phosphorus, commonly expressed as P_2O_5, directly interferes with these mechanisms and is widely recognized as a critical inhibitor of rutilization.

Experimental and conceptual studies of phosphorus-modified TiO_2 systems consistently show that phosphorus-bearing species preferentially segregate at particle surfaces and grain boundaries during thermal treatment, thereby reducing boundary mobility and suppressing coarsening. The formation of Ti–O–P bonds or thin phosphate-rich intergranular films stabilizes the anatase structure and raises the energy barrier for rutile transformation, even at temperatures normally sufficient for complete rutilization in phosphorus-free systems.

As a direct consequence, calcination of TiO_2 precursors with elevated P_2O_5 levels can yield mixed-phase pigments containing both rutile and residual anatase. These biphasic products exhibit inferior optical performance because of reduced refractive-index contrast, altered light-scattering behavior, and poorer dispersibility in coating and polymer matrices (Zhang, J. *et al*., 2024; Yan *et al*., 2024). Industrially, such materials are generally considered unsuitable for high-grade pigment applications, where strict control of phase purity is required rather than reliance on average chemical composition alone.

Despite the central importance of this phenomenon, the literature remains fragmented regarding quantitative thresholds linking P_2O_5 content to rutilization failure. Many studies report phosphorus concentrations without correlating them with phase evolution outcomes, while others investigate phosphorus-doped TiO_2 primarily from a functional-materials perspective rather than a pigment-performance perspective. This disconnect highlights the need to reinterpret existing data through a pigment-oriented framework, where the critical criterion is the ability to achieve complete rutilization during calcination.

The effect of phosphorus on TiO_2 phase evolution is most clearly observed during calcination, when residual P_2O_5 can fundamentally alter the anatase-to-rutile transformation pathway. To clarify this mechanism, Figure 4 schematically contrasts the calcination behavior of phosphorus-free and phosphorus-bearing TiO_2 systems.

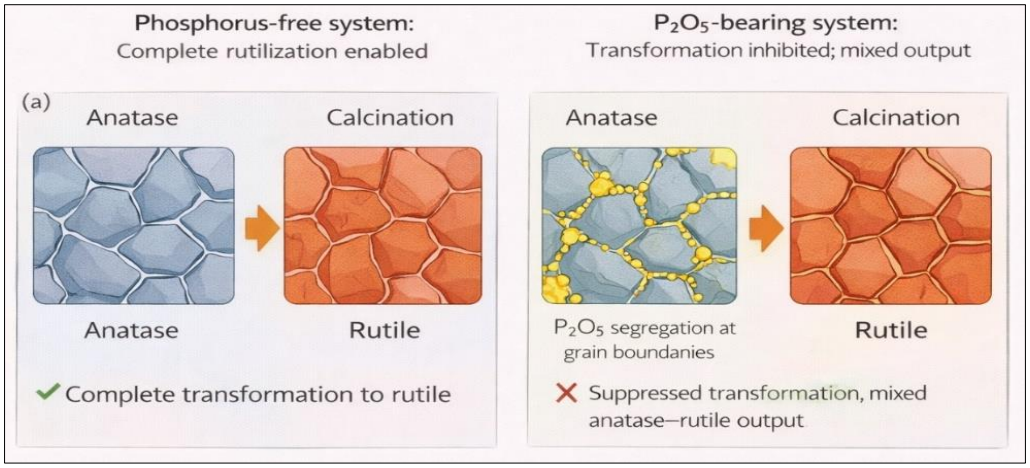

Fig 1: Schematic representation of anatase-to-rutile transformation during calcination: (a) phosphorus-free system enabling complete rutilization; (b) P_2O_5-bearing system showing grain-boundary segregation, suppressed transformation, and mixed anatase–rutile output. Adapted from: Thambiliyagodage *et al*. (2021).

Figure 4 shows that, in the absence of phosphorus, anatase particles fully transform to rutile during calcination, producing a single-phase pigment with the optical and dispersive properties required for commercial TiO_2 products. In contrast, when P_2O_5 is present, phosphorus preferentially segregates at grain boundaries and particle interfaces, hindering atomic rearrangement and suppressing rutilization. The resulting mixed anatase–rutile product exhibits inferior pigment performance and is therefore considered non-commercial. This mechanistic distinction explains why even low residual phosphorus levels can critically compromise pigment quality, regardless of the upstream processing route.

Beyond qualitative mechanistic descriptions, the industrial relevance of phosphorus in TiO_2 phase evolution becomes clearer when rutilization behavior is considered within the calcination temperature window typically used in pigment manufacture (≈850–1050 °C). A conceptual representation of the rutile fraction as a function of calcination temperature (Figure 5) provides a practical framework for illustrating how residual P_2O_5 suppresses phase transformation under conditions representative of commercial rotary kilns and fluidized-bed calciners.

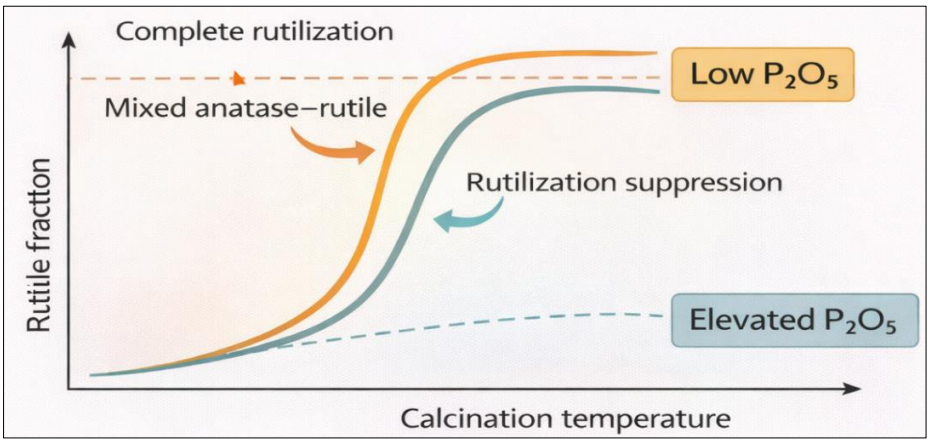

Fig 2: Conceptual plot of rutile fraction versus calcination temperature for TiO_2 with low and elevated P_2O_5 contents, illustrating rutilization suppression. Adapted from: Thambiliyagodage *et al*. (2021).

As shown in Figure 5, phosphorus-lean TiO_2 precursors exhibit a rapid rise in the rutile fraction between approximately 850 and 950 °C, reaching near-complete rutilization within the standard industrial calcination range. In contrast, TiO_2 containing elevated P_2O_5 shows a delayed onset of transformation, a lower transformation rate, and incomplete rutilization even at temperatures approaching or exceeding 1050 °C.

This behavior reflects the segregation of phosphorus at grain boundaries and interfaces, which impedes atomic rearrangement and slows rutile grain growth. From an industrial standpoint, the conceptual trend indicates that increasing calcination temperature beyond conventional operating limits is not an effective compensatory strategy. Instead, higher temperatures tend to increase energy consumption, sintering, and particle coarsening without achieving pigment-grade phase purity. Consequently, effective upstream phosphorus control is a prerequisite for reliable rutilization within practical industrial temperature constraints.

Section 5 shows that phosphorus compromises TiO_2 pigment quality at multiple levels, culminating in inhibited rutile formation during calcination and the production of non-commercial mixed-phase pigments. These impacts underscore that phosphorus control must occur upstream, at the ore and feedstock preparation stages, rather than being addressed solely through downstream process adjustments. Consequently, Section 6 examines physical beneficiation routes for phosphorus removal, focusing on how effectively mineralogical liberation and separation strategies can reduce phosphorus inputs before chemical or thermochemical processing.

6. Physical beneficiation routes for phosphorus removal

Physical beneficiation is typically the first intervention for phosphorus control in titanium ores, targeting the rejection of phosphorus-bearing phases before chemical or thermochemical processing. The effectiveness of these approaches is governed primarily by mineralogical occurrence, liberation characteristics, and contrasts in density or magnetic properties between phosphate phases and Ti-bearing minerals. Although attractive because of their relatively low operating costs and minimal reagent consumption, the applicability of physical routes to phosphorus removal remains strongly feed-dependent and is often constrained by textural complexity.

6.1. Gravity separation

Gravity separation exploits density contrasts between titanium minerals and gangue phases and is widely used to upgrade heavy mineral sands and titaniferous ores. Phosphate minerals such as apatite generally have lower densities than ilmenite and rutile, allowing partial rejection during gravity concentration. However, mineralogical studies show that phosphorus-bearing phases frequently occur as fine-grained inclusions or composite particles, which markedly reduces the effectiveness of density-based separation (Mandende & Mothupi, 2024; Khedr *et al*., 2024).

Empirical evidence from complex Fe–Ti–P systems indicates that gravity separation achieves meaningful phosphorus reduction only when apatite is liberated and relatively coarse, with performance declining sharply as particle size decreases or intergrowth complexity increases (Alfonso *et al*., 2020; Üçerler-Çamur *et al*., 2025). Consequently, gravity circuits are rarely sufficient to meet pigment-grade phosphorus specifications and are primarily used for pre-concentration rather than as standalone dephosphorization steps.

The data in Table 6 confirm that gravity separation can achieve meaningful phosphorus rejection only under favorable mineralogical conditions, particularly when apatite occurs as coarse, liberated grains. In most industrially relevant titanium ores, phosphorus is hosted in fine inclusions or composite particles, limiting gravity separation to a pre-concentration role rather than a standalone dephosphorization solution capable of meeting pigment-grade specifications.

Table 6: Reported performance of gravity separation for phosphorus rejection in titanium ores: feed characteristics, particle size range, and achievable P reduction

Ore / feedstock type	Main P host mineral	Typical particle size range	Gravity separation unit	Achievable P or P_2O_5 reduction	Key limitations
Ilmenite-rich heavy mineral sand	Apatite (discrete grains)	>150 µm	Spirals, shaking tables	Moderate (≈20–40%)	Effective only for coarse, liberated apatite
Titaniferous magnetite ore	Apatite (intergrowths)	75–150 µm	Dense media separation	Low to moderate (≤25%)	Composite particles reduce density contrast
Fe–Ti–P complex ore	Apatite inclusions in Fe–Ti oxides	<75 µm	Spirals + scavenging tables	Low (<15%)	Fine inclusions and poor liberation
Altered ilmenite / leucoxene	Residual apatite, microdomains	<106 µm	Gravity pre-concentration	Marginal (<10%)	Textural locking dominates performance
Vanadium–titanium magnetite tailings	Apatite + mixed phosphates	38–150 µm	Enhanced gravity concentrators	Moderate locally (up to ~30%)	Strong sensitivity to size classification

6.2. Magnetic separation

Magnetic separation is widely used in titanium ore processing because of differences in magnetic susceptibility among ilmenite, titanomagnetite, and gangue minerals. Phosphorus-bearing phases are generally weakly magnetic or non-magnetic; thus, phosphorus rejection by magnetic separation is indirect and governed by the degree of association between phosphate minerals and magnetic Fe–Ti oxides.

Studies of vanadium–titanium magnetite and ilmenite-rich systems show that low- and high-intensity magnetic separation can redistribute phosphorus among products, but complete rejection is uncommon when apatite occurs as inclusions within magnetic host grains (Xiao *et al*., 2020; Zhai *et al*., 2020). In some cases, phosphorus may even concentrate in Ti-rich fractions when phosphate phases preferentially associate with ilmenite rather than silicate gangue (Zeng *et al*., 2022; Khedr *et al*., 2024).

Overall, these results confirm that magnetic separation performance for phosphorus control is governed primarily by textural associations rather than intrinsic magnetic properties, underscoring the need for detailed mineralogical assessment during circuit design.

Figure 6 shows that phosphorus removal by magnetic separation is inherently indirect and governed by mineralogical associations rather than intrinsic magnetic properties. When apatite occurs as liberated, nonmagnetic particles, it can be efficiently rejected to the tailings. In contrast, phosphate inclusions encapsulated within ilmenite or titanomagnetite grains are carried into the magnetic concentrate, resulting in phosphorus enrichment of the Ti-rich product.

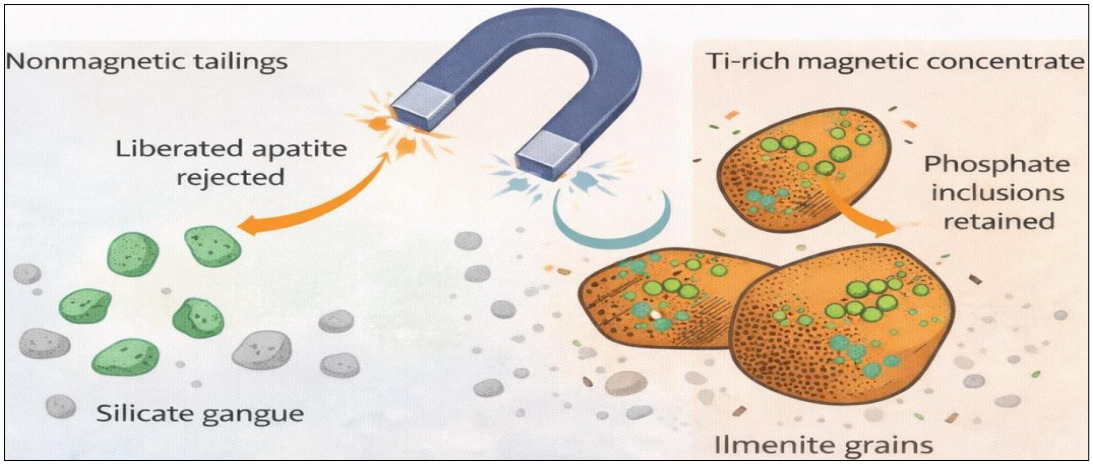

Fig 3: Conceptual illustration of phosphorus deportment during magnetic separation, showing liberated apatite rejection versus phosphate inclusions retained within ilmenite grains. Adapted from Xiao *et al*. (2020), Zhai *et al*. (2020), Zeng *et al*. (2022), and Khedr *et al*. (2024).

This conceptual framework explains why magnetic separation often redistributes rather than eliminates phosphorus and, in some cases, increases P levels in upgraded concentrates. From an industrial perspective, the figure reinforces that magnetic circuits should be designed primarily for iron–titanium upgrading, with phosphorus control treated as a secondary, highly feed-dependent outcome.

6.3. Flotation of phosphorus-bearing phases

Flotation provides higher selectivity for phosphorus removal than gravity or magnetic separation, particularly when phosphate minerals can be rendered hydrophobic via tailored reagent schemes. Direct flotation of apatite has been demonstrated in phosphorus-bearing vanadium–titanium magnetite tailings and complex oxide systems, yielding higher phosphorus rejection under favorable liberation conditions (Xiao *et al*., 2020).

In ilmenite processing, flotation performance is strongly governed by surface chemistry, reagent adsorption, and competitive interactions between collectors and Fe–Ti oxide discrete phosphate particles can be efficiently removed, effectiveness declines sharply when phosphorus occurs as ultra-fine inclusions or is structurally bound within Ti-bearing minerals. Increased ore complexity also leads to higher reagent consumption and reduced selectivity (Zhai *et al*., 2020; Luo *et al*., 2020).

From a pigment-oriented perspective, flotation should be regarded as a conditional dephosphorization step that can

reduce phosphorus input but is rarely sufficient on its own to meet strict pigment-grade P_2O_5 limits.

The data in Table 7 show that flotation can achieve higher phosphorus rejection than gravity or magnetic separation when apatite occurs as liberated particles and reagent selectivity is well controlled. However, performance declines inclusions or is structurally bound within Ti-bearing minerals. From an industrial standpoint, flotation is therefore best deployed as a conditional upstream control step rather than as a standalone solution capable of ensuring compliance with pigment-grade phosphorus specifications.

Table 7: Comparison of flotation-based phosphorus removal strategies: collectors, target phases, typical phosphorus rejection, and key limitations. Adapted from Xiao *et al*. (2020); Fang *et al*. (2020); Zhang, H. *et al*. (2022); Zhai *et al*. (2020); Luo *et al*. (2020).

Ore / feedstock type	Target P-bearing phase	Main collector / reagent scheme	Typical P or P_2O_5 rejection	Key limitations
Vanadium–titanium magnetite tailings	Apatite (liberated)	Fatty acids, hydroxamates	High (≈40–70%)	Requires good liberation; sensitive to slime coating
Ilmenite-rich ore	Apatite (discrete grains)	Fatty acids + modifiers	Moderate (≈30–50%)	Competitive adsorption on Fe–Ti oxides
Complex Fe–Ti–P ore	Mixed phosphate phases	Mixed collectors	Moderate to low (≤40%)	Poor selectivity in complex mineralogy
Altered ilmenite / leucoxene	Residual apatite, fine phosphates	Fatty acids, sulfonates	Low (<25%)	Ultra-fine inclusions and high reagent consumption
Complex oxide tailings	Apatite + secondary phosphates	Customized reagent suites	Variable (20–60%)	Froth instability and reagent cost escalation

6.4. Performance limits and scale-up challenges

Despite their industrial maturity, physical beneficiation methods have inherent limitations for phosphorus removal from titanium ores. Across gravity separation, magnetic separation, and flotation, liberation constraints consistently dominate performance, often outweighing equipment selection or reagent optimization (Alfonso *et al*., 2020; Üçerler-Çamur *et al*., 2025). Fine phosphate inclusions, complex intergrowths, and heterogeneous microscale phosphorus distribution limit the maximum dephosphorization achievable by physical means alone.

At scale-up, additional challenges arise from ore mineralogical variability, sensitivity to particle-size distribution, and the trade-off between phosphorus rejection and titanium recovery. Aggressive separation may lower phosphorus levels but at the expense of unacceptable Ti losses, undermining process economics (Lv *et al*., 2020; Xu & Wang, 2025). Moreover, physical beneficiation does not prevent phosphorus redistribution during subsequent thermal or chemical processing, where residual phosphorus may reappear as a critical impurity during calcination.

Consequently, while physical beneficiation remains an effective front-end strategy for reducing phosphorus loading, it is insufficient as a standalone solution for producing pigment-grade feedstocks. Its primary role is to condition the feed before more selective downstream treatments rather than to meet final phosphorus specifications.

From an operational perspective, physical beneficiation routes consistently reach a performance ceiling when phosphorus-bearing apatite occurs as inclusions or intergrowths below the practical liberation size (typically <20–30 μm). Beyond this size, further grinding yields marginal gains in phosphorus rejection while disproportionately increasing titanium losses and energy consumption. As a result, physical beneficiation becomes ineffective as a standalone strategy for meeting pigment-grade phosphorus specifications.

Section 6 shows that physical beneficiation can partially reduce phosphorus content but is fundamentally constrained by mineralogical associations, liberation, and scale-up limitations. To achieve the low phosphorus levels required for pigment-grade TiO_2 production, more selective approaches are necessary. Accordingly, Section 7 examines hydrometallurgical dephosphorization strategies, focusing on acid and alkaline leaching systems, hybrid pre-treatments, and their ability to decouple phosphorus removal from titanium recovery.

7. Hydrometallurgical dephosphorization strategies

Hydrometallurgical processing offers greater chemical selectivity than physical beneficiation and has therefore been extensively explored for phosphorus removal from titanium ores and upgraded feedstocks. Acidic, alkaline, and hybrid leaching routes can dissolve phosphorus-bearing phases or transfer phosphorus into solution, enabling lower residual P_2O_5 levels than physical methods alone. These benefits, however, are offset by challenges related to titanium co-dissolution, reagent intensity, effluent management, and compatibility with downstream pigment production.

7.2. Acid leaching systems

Acid leaching with hydrochloric acid (HCl) and sulfuric acid (H_2SO_4) is the most extensively studied hydrometallurgical route for titanium ores. In ilmenite and altered ilmenite systems, acid leaching can dissolve iron-bearing phases and associated phosphates, enabling partial phosphorus removal from the solid residue (Anggraeni *et al*., 2023; Dubenko *et al*., 2020). Mixed-acid systems and optimized acid concentrations have been investigated to enhance phosphorus dissolution while limiting titanium losses (Long *et al*., 2025). HCl leaching is particularly attractive for integration with chloride-route processing because it supports downstream solvent extraction and titanium purification (Ahn & Lee, 2021; Kordzadeh-Kermani *et al*., 2020). However, phosphorus dissolution in acidic media is often poorly selective, and phosphate species form stable solution complexes that complicate liquor purification. In sulfate-route contexts, H_2SO_4 leaching may redistribute phosphorus into solid residues or recycled liquors, increasing the risk of impurity accumulation if purge streams are not carefully controlled (Tahooni Bonab *et al*., 2025).

The data in Table 8 show that acid leaching can achieve substantially higher phosphorus removal than physical beneficiation methods, particularly in ilmenite-based feeds.

However, phosphorus dissolution is often accompanied by non-negligible titanium losses and the formation of phosphate-bearing liquors that require further purification. When phosphorus removal depends on dissolving refractory phosphate phases embedded in Ti-bearing minerals, increases in acid concentration, temperature, or residence time rapidly shift the process window from selective dephosphorization to bulk titanium dissolution, imposing a fundamental limit on the industrial viability of aggressive acid leaching. From a pigment-production perspective, these trade-offs limit the standalone applicability of acid leaching and underscore the need for careful integration with downstream recovery, purification, and waste-management strategies.

Table 8: Acid leaching systems for phosphorus removal from titanium ores: acid type, operating conditions, phosphorus removal efficiency, and reported titanium dissolution. Adapted from Dubenko *et al*. (2020); Ahn & Lee (2021); Kordzadeh-Kermani *et al*. (2020); Anggraeni *et al*. (2023); Long *et al*. (2025); Tahooni Bonab *et al*. (2025).

Ore / feedstock type	Acid system	Typical operating conditions*	Phosphorus (P or P_2O_5) removal	Titanium dissolution	Key observations
Ilmenite concentrate	HCl	4–8 M; 80–100 °C	Moderate–high (≈40–70%)	Moderate (≈5–15%)	Good Fe and P removal; Ti losses increase at high acidity
Altered ilmenite	H_2SO_4	20–30 wt%; 90–110 °C	Moderate (≈30–60%)	Low–moderate (≤10%)	Risk of P accumulation in recycled liquors
Ilmenite	Mixed HCl–H_2SO_4	Variable ratios; 80–100 °C	High (up to ≈75%)	Moderate (≈10–20%)	Improved P dissolution but reduced selectivity
Ilmenite slag / Ti-rich residue	HCl	6–10 M; elevated temperature	Moderate (≈35–60%)	Moderate	Phosphate complexation complicates purification
Complex Ti-bearing ore	H_2SO_4	Concentrated acid; >90 °C	Variable (20–50%)	Low–moderate	Strong dependence on mineralogy and pretreatment

*Typical conditions reported in the literature; values vary with mineralogy, particle size, and leaching time.

7.3. Alkaline and salt-based leaching

Alkaline leaching systems using NaOH or Na_2CO_3 have been proposed to selectively decompose phosphate-bearing phases and condition the mineral matrix prior to acid leaching. Alkaline roasting followed by leaching has been effective in disrupting refractory phases in anatase- and ilmenite-rich ores, thereby facilitating subsequent phosphorus removal (De Oliveira *et al*., 2023; Pysarenko *et al*., 2023). In some cases, alkaline treatment promotes the formation of soluble phosphate species that can be separated from titanium-rich residues (Azamat *et al*., 2021).

However, alkaline routes are typically energy-intensive and may introduce sodium into solid residues, which can harm downstream pigment processing if not properly controlled. Phosphorus removal efficiency is also highly sensitive to roasting temperature, reagent dosage, and mineralogical context, leading to wide variability in reported performance and complicating scale-up (Supriyatna *et al*., 2023; Spencer *et al*., 2025). Under these conditions, alkaline routes have a narrow operational window, where insufficient activation limits phosphorus removal, while excessive roasting or alkali dosage causes sodium contamination and progressive degradation of downstream pigment performance.

Figure 7 shows that during alkaline roasting with NaOH or Na_2CO_3, phosphorus-bearing phases convert to sodium phosphate species, which can then be leached and separated from the titanium-rich solid. While this transformation enhances phosphorus removal, incomplete washing or insufficient downstream treatment may leave residual sodium in the solid phase. From a pigment-production perspective, such sodium carryover is undesirable because it can adversely affect downstream acid digestion, calcination behavior, and pigment quality. The schematic underscores that alkaline routes require careful control of roasting severity, leaching efficiency, and residue conditioning to balance phosphorus removal against the introduction of secondary impurities.

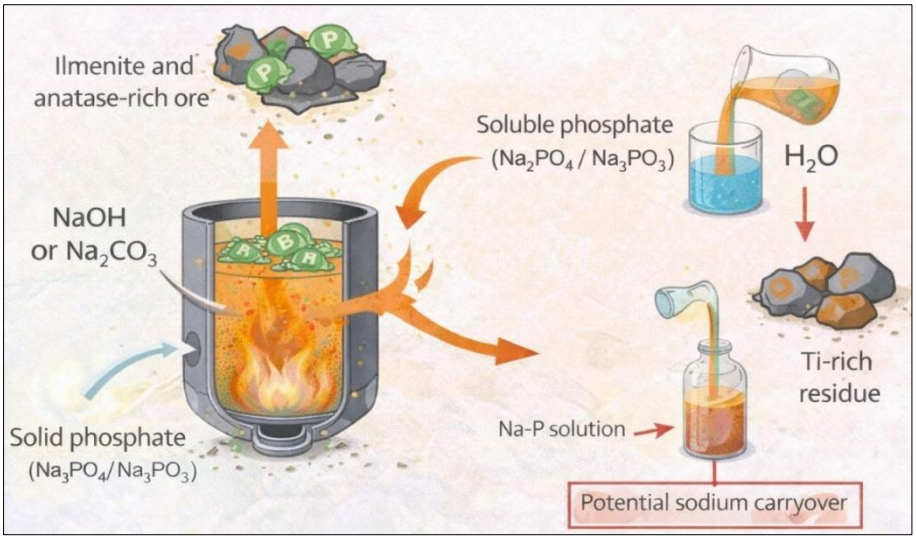

Fig 4: Schematic of alkaline roasting and leaching routes highlighting phosphorus transformation and potential sodium carryover. Adapted from De Oliveira *et al*. (2023); Pysarenko *et al*. (2023); Azamat *et al*. (2021); Supriyatna *et al*. (2023); Spencer *et al*. (2025).

7.4. Hybrid approaches

Hybrid hydrometallurgical approaches combine thermal activation with subsequent leaching or integrate reductive and oxidative pre-treatments to enhance phosphorus removal. Thermal activation methods—including mechanical activation, microwave treatment, and controlled roasting—have been shown to increase mineral reactivity and disrupt phosphate-bearing microstructures, thereby improving leaching kinetics and impurity rejection (Luo *et al*., 2020; Wang & Jiang, 2024).

Reductive pre-treatments may promote phosphorus migration into iron-rich phases that can be preferentially leached or separated, whereas oxidative treatments can convert phosphorus into more soluble species (Daba *et al*., 2022; Chen *et al*., 2024). Although these hybrid routes often achieve higher phosphorus removal than single-step leaching, they also introduce greater flowsheet complexity, higher capital intensity, and stronger feed dependency, which can limit their robustness and industrial scalability.

As shown in Figure 8, hybrid routes use thermal activation to overcome liberation and reactivity constraints that limit conventional leaching. By disrupting phosphate-bearing microstructures or altering phosphorus partitioning between phases, these flowsheets can achieve incremental phosphorus removal with improved selectivity. However, the benefits of hybridization must be weighed against increased process complexity, energy demand, and capital intensity. From a pigment-oriented perspective, such routes are most attractive when they demonstrably reduce residual P_2O_5 to levels compatible with complete rutilization while maintaining acceptable titanium recovery and downstream process compatibility.

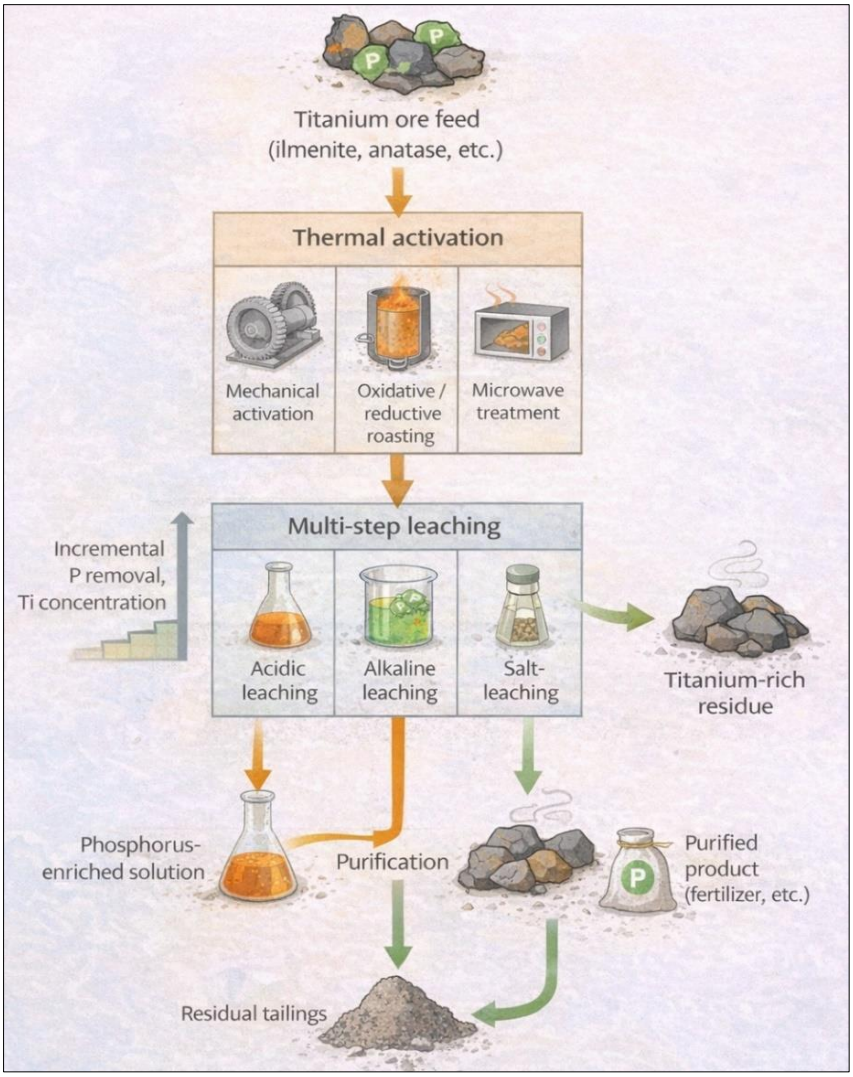

Fig 5: Conceptual hybrid hydrometallurgical flowsheet combining thermal activation and leaching for phosphorus removal from titanium ores. Adapted from: Luo *et al*. (2020); Wang & Jiang (2024); Daba *et al*. (2022); Chen. *et al*. (2024); De Oliveira *et al*. (2023).

7.5. Critical assessment

From a critical perspective, hydrometallurgical dephosphorization strategies generally achieve higher phosphorus removal efficiencies than physical beneficiation, particularly for finely disseminated or chemically bound phosphorus. However, this selectivity is often offset by titanium losses under the aggressive conditions required to dissolve refractory phosphate phases (Anggraeni *et al*., 2023; Tahooni Bonab *et al*., 2025). High reagent consumption and energy demand—especially in alkaline roasting and hybrid routes—further constrain economic viability.

Environmental considerations add another layer of complexity. Both acidic and alkaline leaching produce substantial effluent volumes containing dissolved phosphorus, iron, and residual reagents, necessitating effective treatment and disposal (Luyckx & Van Caneghem, 2022). Moreover, inconsistent reporting of phosphorus mass balances and effluent chemistry across studies limits direct

comparability and obscures the true sustainability of proposed routes (Mogashane *et al*., 2025).

Critically, hydrometallurgical selectivity is constrained by a narrow process window: beyond moderate acid strength, temperature, or residence time, phosphorus removal rapidly becomes dominated by titanium loss. Under such conditions, incremental gains in P_2O_5 removal come at the expense of substantially reduce phosphorus levels but often at the expense of titanium recovery, reagent use, and effluent management complexity. An alternative is offered by thermochemical and pyrometallurgical approaches, in which phosphorus may partition into metal or slag phases during high-temperature processing, potentially enabling simultaneous removal of iron, phosphorus, and other deleterious elements. Accordingly, Section 8 examines pyrometallurgical and thermochemical routes for phosphorus control in titanium feedstocks, with emphasis on slag chemistry, element partitioning, and implications for pigment-grade TiO_2 production.

8. Pyrometallurgical and thermochemical approaches

Pyrometallurgical and thermochemical routes offer an alternative paradigm for phosphorus control in titanium feedstocks by exploiting high-temperature reactions to redistribute phosphorus among the metal, slag, and, in limited cases, the gas phase. Unlike physical or hydrometallurgical methods, these approaches rely on thermodynamic driving forces, enabling the simultaneous modification of multiple impurities and phase assemblages. Their relevance is particularly pronounced for ilmenite concentrates and complex Fe–Ti ores subjected to slag-based upgrading prior.

8.1. Carbothermic reduction and smelting

Carbothermic reduction and smelting are widely used for ilmenite concentrates to remove iron and produce TiO_2-rich slags suitable for further upgrading. During smelting, phosphorus behavior is governed by its partitioning between metallic iron and oxide slag phases, which is strongly influenced by slag basicity, oxygen potential, and temperature. Thermodynamic analyses and industrial observations indicate that, under sufficiently reducing conditions, phosphorus preferentially partitions into the metallic phase, enabling partial dephosphorization of the slag (Zhang *et al*., 2022; Zeng *et al*., 2022).

Phosphorus partitioning, however, is inherently incomplete. Residual P_2O_5 may remain dissolved in the slag matrix or be incorporated into complex oxide structures, particularly when smelting conditions are optimized primarily for iron removal rather than impurity control (Subasinghe & Ratnayake, 2023; Qu *et al*., 2024) [51]. In addition, competing reactions involving vanadium and other multivalent elements can constrain phosphorus transfer by altering oxygen potential and slag chemistry (Wang *et al*., 2025). As a result, carbothermic smelting can significantly reduce phosphorus input into pigment feedstocks but rarely achieves complete dephosphorization.

In practice, phosphorus partitioning during smelting is governed primarily by slag basicity and oxygen potential rather than temperature alone. Insufficient basicity or overly oxidizing conditions favor phosphorus retention in Ti-rich slags despite high-temperature operation.

As shown in Figure 9, phosphorus preferentially partitions into the metallic iron phase under sufficiently reducing conditions, driven by its affinity for metal over oxide phases at low oxygen potential. This behavior enables partial dephosphorization of the TiO_2-rich slag intended for downstream upgrading and pigment production. However, some phosphorus may remain dissolved in the slag matrix or incorporated into complex oxide species, particularly when slag chemistry and oxygen potential are optimized primarily for iron removal rather than impurity control. The schematic also highlights the role of competing elements, such as vanadium, which can alter slag structure and oxygen potential, thereby constraining phosphorus transfer efficiency. These interactions explain why carbothermic smelting typically reduces—but does not completely eliminate—phosphorus from titanium feedstocks.

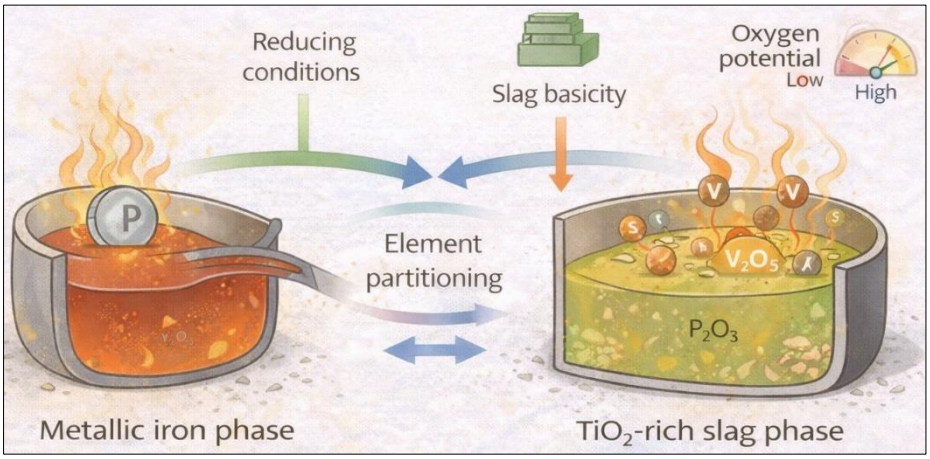

Fig 6: Schematic illustration of phosphorus partitioning between metal and slag during carbothermic smelting of ilmenite concentrates. Adapted from Zhang *et al*. (2022); Zeng *et al*. (2022); Subasinghe and Ratnayake (2023) [51]; Qu *et al*. (2024); Wang. *et al*. (2025).

8.2. Production of Ti-rich slags

The production of Ti-rich slags via controlled smelting is among the most industrially relevant thermochemical strategies for impurity control in titanium feedstocks. These slags typically contain 70–90 wt% TiO_2 and enable the simultaneous removal of iron and partial rejection of deleterious elements, including phosphorus and vanadium (Qu *et al*., 2024; Spencer *et al*., 2025). From a pigment-production perspective, Ti-rich slags offer two key advantages: a reduced impurity burden and enhanced chemical reactivity relative to natural rutile.

Phosphorus removal during slag production is strongly

governed by slag composition and basicity. Slags engineered to promote phosphorus partitioning into the metallic phase or into discrete phosphate-rich domains can achieve lower residual P_2O_5 levels than untreated ilmenite concentrates (Subasinghe & Ratnayake, 2023) [51]. At the same time, vanadium and other redox-sensitive impurities may be reduced and transferred to the metal, further improving the slag's suitability for downstream processing (Zhang *et al*., 2022).

Nevertheless, the literature reports substantial variability in slag compositions and impurity levels, reflecting differences in furnace design, operating conditions, and feed mineralogy. Crucially, high TiO_2 content alone does not guarantee pigment-grade suitability; residual phosphorus, even at low concentrations, can still inhibit rutilization during calcination, underscoring the need for slag design criteria explicitly aligned with pigment performance rather than bulk chemistry alone (Qu *et al*., 2024).

Controlled smelting routes produce a range of Ti-rich slags whose suitability for pigment production depends not only on TiO_2 grade but also on residual levels of redox-sensitive and calcination-critical impurities, particularly phosphorus and vanadium. Although smelting effectively removes iron and can partially partition phosphorus into the metallic phase, significant variability persists in residual P_2O_5 and V_2O_5 contents as a function of slag chemistry, basicity, and operating conditions.

These observations indicate that high TiO_2 content alone is insufficient to guarantee pigment-grade performance, and that slag design criteria must explicitly account for phosphorus behavior to ensure successful downstream calcination.

Table 9 summarizes representative compositions of Ti-rich slags reported in the literature and highlights their practical implications for downstream sulfate- and chloride-route pigment processing, with an emphasis on rutilization performance and impurity-related risks.

Table 9: Typical compositions of Ti-rich slags produced by smelting: TiO_2 content, residual P_2O_5 and V_2O_5, and implications for pigment processing. Adapted from: Subasinghe & Ratnayake (2023) [51]; Qu *et al*. (2024); Zhang *et al*. (2022); Spencer *et al*. (2025).

Slag type / source	TiO_2 (wt%)	Residual P_2O_5 (wt%)	Residual V_2O_5 (wt%)	Key implications for pigment processing
Standard ilmenite smelting slag	70–75	0.05–0.20	0.3–1.0	Suitable for sulfate route; residual P_2O_5 may hinder complete rutilization if not further treated
High-TiO_2 smelting slag (optimized)	80–85	0.02–0.08	0.2–0.6	Improved chloride-route compatibility; reduced P_2O_5 lowers risk of calcination inhibition
Premium Ti-rich slag (selective smelting)	85–90	<0.02	<0.3	Near-pigment-grade feedstock; enhanced rutilization kinetics and phase purity
Vanadium-bearing Ti slag	75–85	0.05–0.15	1.0–3.0	Requires V control to avoid redox interference; P_2O_5 still critical for calcination behavior
Low-basicity Ti slag	70–80	0.10–0.30	0.3–1.2	Higher residual P_2O_5; increased risk of mixed anatase–rutile output
Slag from complex Fe–Ti–V ores	75–85	0.08–0.25	1.5–4.0	Phosphorus and vanadium co-control required; pigment suitability strongly process-dependent

Note: Reported ranges reflect variability in feed mineralogy, furnace design, slag basicity, and oxygen potential. Residual P_2O_5 values above ~0.05 wt% are frequently associated with suppressed rutilization during calcination.

In pyrometallurgical upgrading, phosphorus removal is not an inherent outcome but a design-dependent variable governed primarily by slag basicity, oxygen potential, and temperature. When smelting conditions are optimized solely for iron removal or TiO_2 enrichment, phosphorus partitioning into the metal remains incomplete, yielding Ti-rich slags that may still fail pigment-oriented calcination criteria.

8.3. Oxidative and controlled-atmosphere treatments

Oxidative and controlled-atmosphere thermochemical treatments have been proposed as complementary strategies for phosphorus control, particularly as pre- or post-smelting steps. In theory, phosphorus volatilization as P_2O_5 or sub-oxides could enable direct removal; however, thermodynamic constraints severely limit this mechanism under practical operating conditions. Phosphorus oxides have low vapor pressures at the temperatures typically used in titanium processing, and strong interactions with slag-forming oxides further suppress volatilization.

Controlled-atmosphere treatments may still influence phosphorus speciation and distribution within solid phases. Oxidative roasting can convert reduced phosphorus species into more stable phosphate forms, facilitating subsequent removal via slagging or leaching, whereas reductive atmospheres favor phosphorus partitioning into the metal during smelting (Daba *et al*., 2022, Chen. *et al*., 2024). These treatments are therefore best understood as enablers of phosphorus redistribution rather than standalone removal techniques.

From a process-integration standpoint, the main challenge is balancing impurity control with energy consumption and furnace operability. Excessive oxidation or reduction may compromise slag fluidity, refractory stability, or downstream reactivity, thereby limiting the practical applicability of such approaches without careful thermodynamic and kinetic optimization (Subasinghe & Ratnayake, 2023) [51].

Section 8 shows that pyrometallurgical and thermochemical approaches can effectively redistribute phosphorus during high-temperature processing, particularly by partitioning it into metallic phases and through controlled slag design. However, their success depends heavily on operating conditions, slag chemistry, and integration with downstream processing, and residual phosphorus may still persist at levels detrimental to pigment quality. These observations highlight the need for a comparative evaluation of all dephosphorization routes, considering not only phosphorus

removal efficiency but also titanium recovery, process complexity, and pigment performance. Accordingly, Section 9 provides a comparative assessment of physical, hydrometallurgical, and thermochemical dephosphorization strategies.

9. Comparative evaluation of dephosphorization routes

The dephosphorization strategies reviewed in Sections 6–8 differ markedly in effectiveness, selectivity, and industrial applicability. A comparative evaluation is therefore essential to identify which routes are technically viable for producing pigment-grade TiO_2 feedstocks, where the ultimate performance criterion is not phosphorus removal alone but the ability to enable complete rutilization during calcination without compromising titanium recovery or process sustainability.

When evaluated against industrial calcination windows (typically 850–1050 °C), the effectiveness of dephosphorization routes diverges more sharply than bulk chemical analyses alone suggest. Routes that reduce total P_2O_5 but fail to modify phosphorus speciation or microscale distribution often remain insufficient to ensure complete rutilization.

9.1. Phosphorus removal efficiency versus titanium recovery

Across the reviewed routes, physical beneficiation consistently shows the lowest phosphorus removal efficiency, particularly for finely disseminated or structurally bound phosphorus. Although gravity separation, magnetic separation, and flotation can reduce phosphorus inputs, residual P_2O_5 levels often remain above thresholds that impair rutilization, limiting their effectiveness as standalone solutions despite generally high titanium recovery (Alfonso *et al*., 2020; Üçerler-Çamur *et al*., 2025; Zhai *et al*., 2020).

Hydrometallurgical strategies achieve higher phosphorus removal efficiency when phosphate phases are chemically accessible. However, this improved selectivity is often offset by titanium co-dissolution, increased reagent consumption, and complex effluent streams. Aggressive leaching conditions required to extract refractory phosphorus-bearing phases can significantly reduce overall titanium yield, particularly for upgraded feedstocks (Anggraeni *et al*., 2023; Tahooni Bonab *et al*., 2025; Mogashane *et al*., 2025).

Pyrometallurgical and thermochemical approaches—especially smelting-based routes—offer a more balanced compromise by promoting phosphorus partitioning into metallic phases while retaining titanium in Ti-rich slags. Although complete phosphorus elimination is uncommon, careful control of slag chemistry can reduce residual P_2O_5 to levels compatible with downstream processing and pigment production (Subasinghe & Ratnayake, 2023 [51]; Qu *et al*., 2024).

9.2. Impact on rutilization behavior

The comparative impact of dephosphorization routes on the anatase-to-rutile transformation is a key differentiator that remains insufficiently addressed in the literature. Physical beneficiation lowers phosphorus loading but does not alter its chemical form; as a result, residual P_2O_5 may still segregate at grain boundaries during calcination, inhibiting rutilization (Alfonso *et al*., 2020; Üçerler-Çamur *et al*., 2025). Hydrometallurgical routes can achieve deeper phosphorus removal, yet incomplete purification or phosphate reprecipitation may still compromise phase transformation if process control is inadequate (Anggraeni *et al*., 2023; Tahooni Bonab *et al*., 2025).

Thermochemical routes influence rutilization more indirectly by redistributing phosphorus away from the TiO_2 precursor phase. Ti-rich slags produced under optimized smelting conditions generally exhibit enhanced reactivity and reduced susceptibility to phosphorus-induced anatase stabilization, provided residual P_2O_5 is sufficiently low (Subasinghe & Ratnayake, 2023 [51]; Qu *et al*., 2024). From a pigment-performance perspective, controlling phosphorus speciation is therefore as critical as controlling its bulk concentration.

9.3. Process complexity, TRL, and environmental footprint

From an industrial perspective, physical beneficiation routes have the highest technology readiness levels (TRL) and the lowest process complexity, but their limited phosphorus removal capacity restricts their use to early-stage upgrading (Alfonso *et al*., 2020; Üçerler-Çamur *et al*., 2025). Hydrometallurgical routes span a broad TRL range—from laboratory-scale studies to mature industrial leaching operations—but impose significant environmental and operational burdens due to high reagent consumption and effluent generation (Anggraeni *et al*., 2023; Tahooni Bonab *et al*., 2025).

and enable integrated control of phosphorus, along with iron and vanadium removal. Their environmental footprint is dominated by energy use and slag management rather than liquid effluents, representing a fundamentally different sustainability trade-off from chemically intensive leaching processes (Subasinghe & Ratnayake, 2023 [51]; Qu *et al*., 2024).

9.4. Compatibility with sulfate and chloride pigment routes

Compatibility with downstream pigment processes further differentiates dephosphorization strategies. Physical beneficiation is broadly compatible with both sulfate and chloride routes, but its limited phosphorus removal capacity rarely meets the stringent purity requirements of chloride-route feedstocks (Zhai *et al*., 2020; Qu *et al*., 2024). Hydrometallurgical approaches integrate well with sulfate-route processing but may produce residual impurities or chemical species that are incompatible with chloride-route specifications unless additional purification steps are implemented (Anggraeni *et al*., 2023; Tahooni Bonab *et al*., 2025).

Thermochemical upgrading to Ti-rich slags is intrinsically aligned with the chloride process and, in some cases, can also yield highly reactive materials for sulfate digestion. Ultimately, however, route compatibility depends on whether residual phosphorus levels fall below thresholds that impair rutilization during calcination, underscoring the need to assess feedstock quality using pigment-performance criteria rather than bulk chemical assays alone (Subasinghe & Ratnayake, 2023 [51]; Qu *et al*., 2024).

Across the evaluated routes, distinct operational limits emerge. Physical beneficiation saturates at the liberation threshold of phosphorus-bearing phases; hydrometallurgical routes saturate at constraints on titanium loss and effluent management; and thermochemical routes succeed or fail primarily based on slag design rather than on absolute

phosphorus removal efficiency. These limits define the practical envelope for each strategy in pigment-oriented applications.

To enable a clear, pigment-focused comparison of the main dephosphorization strategies, Table 10 summarizes the relative performance of physical beneficiation, hydrometallurgical, and pyrometallurgical/thermochemical routes using criteria that extend beyond phosphorus removal efficiency. In addition to titanium recovery, the table explicitly considers each route's impact on anatase-to-rutile transformation, technology readiness level (TRL), environmental footprint, and compatibility with sulfate and chloride pigment processes. This comparative framework highlights the trade-offs governing industrial route selection and underscores the need to evaluate phosphorus control strategies in terms of downstream pigment performance rather than bulk chemical specifications.

Table 10: Comparative evaluation of phosphorus removal strategies for TiO_2 pigment feedstocks. Adapted from comparative analyses and industrial assessments reported by Zhai *et al*. (2020), Alfonso *et al*. (2020), Subasinghe and Ratnayake (2023) [51], Qu *et al*. (2024), Anggraeni *et al*. (2023), and Tahooni Bonab *et al*. (2025)

Dephosphorization route	Phosphorus removal efficiency (%)	Titanium recovery (%)	Impact on rutilization behavior	Process complexity / TRL	Environmental footprint	Compatibility with sulfate route	Compatibility with chloride route
Physical beneficiation	Low–moderate	High	Limited improvement; residual P_2O_5 remains inhibitory	Low / High TRL	Low	Moderate	Low
Hydrometallurgical	Moderate–high	Moderate	Potentially positive; risk of re-precipitated phosphates	High / Medium TRL	High (effluents)	High	Moderate
Pyrometallurgical / thermochemical	Moderate	High	Indirectly favorable via phosphorus partitioning	High / High TRL	Moderate–high (energy)	Moderate	High

Section 9 shows that no single dephosphorization route optimizes phosphorus removal, titanium recovery, and pigment performance simultaneously. Instead, effective solutions emerge from process integration, in which physical, chemical, and thermochemical strategies are combined based on feedstock mineralogy and downstream pigment requirements. Beyond technical performance, these choices have direct implications for environmental impact, economic viability, and long-term sustainability. Accordingly, Section 10 examines environmental, economic, and sustainability considerations, positioning phosphorus control within the broader framework of responsible and industrially viable TiO_2 pigment production.

10. Environmental, economic, and sustainability considerations

Phosphorus control in titanium feedstocks cannot be evaluated solely by removal efficiency or pigment quality. Each dephosphorization route entails distinct environmental burdens, economic costs, and sustainability implications that must be assessed within the broader context of TiO_2 pigment production, where profitability is highly sensitive to energy demand, reagent intensity, and waste management (Subasinghe & Ratnayake, 2023 [51]; Qu *et al*., 2024).

10.1. Energy demand and CO_2 emissions

Energy demand varies widely across dephosphorization strategies and is a major driver of indirect CO_2 emissions. Physical beneficiation routes typically have the lowest specific energy consumption because they rely primarily on mechanical separation; however, their limited phosphorus removal often requires additional downstream treatments, which erode this advantage (Alfonso *et al*., 2020; Üçerler-Çamur *et al*., 2025).

Hydrometallurgical routes involve moderate energy use for grinding, solution heating, and occasional thermal pre-treatments, with a carbon footprint strongly influenced by upstream reagent production, particularly acids and alkalis (Anggraeni *et al*., 2023; Tahooni Bonab *et al*., 2025). Pyrometallurgical and thermochemical approaches are the most energy-intensive, with direct emissions tied to fossil reductants and electricity use. However, their ability to remove multiple impurities in a single step may partially (Subasinghe & Ratnayake, 2023 [51]; Qu *et al*., 2024).

From an industrial sustainability perspective, the most problematic scenarios are not those with high energy intensity alone, but rather those that combine moderate phosphorus removal with persistent calcination failure, resulting in off-spec pigment production, reprocessing, or waste generation. Phosphorus control, therefore, directly influences both environmental footprint and economic risk.

10.2. Reagent and water consumption

Reagent consumption clearly distinguishes dephosphorization routes. Physical beneficiation requires minimal chemical inputs, whereas hydrometallurgical processes are inherently reagent- and water-intensive. Acidic and alkaline leaching systems generate large volumes of liquid that must be treated or recycled, increasing both operational costs and environmental pressure, particularly in water-constrained regions (Luyckx & Van Caneghem, 2022). Thermochemical routes reduce reliance on aqueous reagents but may require fluxes, reductants, or controlled atmospheres, shifting sustainability concerns toward energy use and solid residue management. From a sustainability standpoint, processes that minimize fresh reagent input and enable closed-loop recycling are inherently more robust (Subasinghe & Ratnayake, 2023) [51].

10.3. Management and valorization of phosphorus-bearing residues

The fate of removed phosphorus is a critical yet often underexplored sustainability issue. In hydrometallurgical systems, phosphorus is commonly transferred to liquid effluents or precipitated as solids that require stabilization or disposal, posing environmental risks related to eutrophication and regulatory compliance if poorly managed (Luyckx & Van Caneghem, 2022).

In contrast, thermochemical routes may concentrate phosphorus in metallic phases or discrete slag fractions, enabling controlled recovery or valorization. Provided contaminant levels are acceptable, phosphorus-bearing slags can serve as secondary raw materials for fertilizers, construction products, or metallurgical fluxes, thereby improving resource efficiency and partially offsetting processing costs (Qu *et al*., 2024).

10.4. Integration with circular economy strategies

From a circular-economy perspective, phosphorus removal should be reframed as a resource management challenge rather than solely a waste-mitigation task. Dephosphorization strategies that enable recovery, reuse, or controlled immobilization of phosphorus are more closely aligned with circular principles. Integrated flowsheets that combine phosphorus control with the recovery of iron, vanadium, or phosphorus-rich by-products offer clear sustainability advantages (Subasinghe & Ratnayake, 2023) [51].

Ultimately, compatibility with existing pigment production infrastructure is crucial for industrial adoption. Incremental improvements that leverage established operations and enable by-product valorization are more likely to achieve large-scale implementation than highly selective, resource-intensive laboratory-scale solutions (Qu *et al*., 2024; Tahooni Bonab *et al*., 2025).

Section 10 shows that phosphorus control in titanium feedstocks involves complex trade-offs among energy use, reagent intensity, waste generation, and opportunities for resource recovery. Although several dephosphorization routes show technical promise, their environmental and economic performance remains strongly context-dependent. These trade-offs highlight persistent knowledge gaps that hinder the translation of laboratory-scale success into industrial robustness. Accordingly, Section 11 identifies key research gaps and outlines future perspectives for advancing phosphorus control strategies aligned with pigment performance, sustainability goals, and circular economy principles.

11. Research gaps and future perspectives

Despite extensive research on phosphorus removal from titanium ores and feedstocks, significant gaps persist that hinder translating dephosphorization strategies into robust, pigment-oriented industrial solutions. Addressing these gaps requires a shift from impurity-centric metrics to performance-driven process design explicitly linked to rutilization behavior and calcination outcomes.

11.1. Lack of standardized phosphorus thresholds linked to rutilization

A major gap is the lack of standardized phosphorus thresholds directly correlated with TiO_2 rutilization performance. While most studies report bulk phosphorus or P_2O_5 content, few establish quantitative relationships among residual phosphorus levels, calcination conditions, and rutile formation. Emphasis is typically placed on chemical removal efficiency, with limited attention to phase transformations during calcination. This limits cross-route comparability and obscures acceptable phosphorus limits for pigment-grade feedstocks. Future studies should systematically link controlled phosphorus concentrations to rutilization kinetics and pigment performance.

11.2. Insufficient coupling of mineralogical characterization and calcination behavior

Although advanced mineralogical tools are increasingly applied to titanium ores, mineralogical characterization is rarely linked to calcination behavior. Microscale phosphorus deportment—such as grain-boundary segregation or inclusion chemistry—is seldom tracked during thermal treatment (Zhukova *et al*., 2022; Üçerler-Çamur *et al*., 2025). This gap limits the mechanistic understanding of phosphorus-induced inhibition of rutilization. Integrated workflows that combine quantitative mineralogy, microstructural analysis, and post-calcination phase characterization are needed to link feedstock texture to pigment performance (Mandende & Mothupi, 2025).

11.3. Limited understanding of phosphorus behavior in Ti-rich slags and synthetic rutile

Despite their central role in pigment production, phosphorus behavior in Ti-rich slags and synthetic rutile remains poorly constrained. Most studies focus on bulk composition and reactivity, overlooking phosphorus incorporation into slag networks or rutile structures and its evolution during downstream processing (Qu *et al*., 2024; Spencer *et al*., 2025). Targeted investigations of phosphorus speciation, partitioning, and thermal stability are required to support rational slag design and quality control.

11.4. Opportunities for hybrid and electrochemical routes

Hybrid flowsheets that integrate physical, hydrometallurgical, and thermochemical steps show promise but remain insufficiently explored at the integrated scale. Electrochemical and electro-assisted routes, in particular, offer potential for selective phosphorus removal with limited titanium losses, yet they currently have low technology readiness levels (Subasinghe & Ratnayake, 2023 [51] ; Stopić *et al*., 2024). These approaches warrant systematic evaluation within pigment-oriented processing frameworks (Rotich *et al*., 2024).

11.5. Toward pigment-oriented process design

Future research must move beyond bulk impurity removal toward pigment-oriented process design. Phosphorus control should be evaluated for its ability to enable complete rutilization, preserve optical and dispersive properties, and integrate sustainably into industrial pigment production. Chemical purity alone is insufficient if phase evolution and microstructure are not controlled (Thambiliyagodage *et al*., 2021; Tahooni Bonab *et al*., 2025). Accordingly, evaluation criteria should prioritize calcination performance, phase purity, and end-use functionality rather than chemical assays alone.

A critical research gap is the lack of operationally defined phosphorus thresholds tied to calcination pass/fail outcomes under industrial conditions. Without these thresholds, laboratory-scale dephosphorization efficiencies are poor predictors of pigment performance and commercial viability.

12. Conclusions

This review shows that phosphorus control is not a marginal quality adjustment but a fundamental process requirement in TiO_2 pigment production. Across ore types, upgrading routes, and pigment processes, residual phosphorus—commonly reported as P_2O_5—emerges as a primary risk factor that

governs calcination performance and commercial viability.

From an industrial standpoint, the relevance of any dephosphorization strategy is ultimately binary: whether the resulting TiO_2 precursor enables complete rutilization within the typical industrial calcination window (≈850–1050 °C). Routes that reduce bulk phosphorus yet fail to suppress P_2O_5 segregation at grain boundaries consistently yield mixed anatase–rutile products and should therefore be regarded as calcination-fail pathways.

A central industrial conclusion is that P_2O_5 directly suppresses the anatase-to-rutile transformation during calcination, even at concentrations typically deemed acceptable under bulk chemical specifications. By segregating at grain boundaries and stabilizing anatase, phosphorus promotes the formation of mixed anatase–rutile products that fail to meet optical, dispersive, and performance standards. These materials are non-commercial, regardless of upstream titanium grade or recovery efficiency.

Evaluation of dephosphorization routes shows that phosphorus must be addressed upstream and strategically, rather than corrected through downstream process adjustments. Physical beneficiation alone rarely meets phosphorus thresholds compatible with reliable rutilization. Hydrometallurgical routes offer higher selectivity but entail significant trade-offs in titanium loss, reagent intensity, and effluent management. Pyrometallurgical upgrading to Ti-rich slags enables partial redistribution of impurities and aligns well with chloride-route feedstocks, but requires explicit slag design criteria tied to phosphorus behavior.

The most robust industrial pathway is integrated dephosphorization strategies that combine physical, chemical, and thermochemical operations and optimize them against pigment-oriented performance metrics rather than solely on bulk impurity removal. Feedstock qualification should therefore be based on demonstrated rutilization behavior under industrial calcination conditions, not solely on chemical assays.

Ultimately, phosphorus control must be treated as an engineering constraint defined by calcination performance rather than as a secondary compositional adjustment, if TiO_2 pigment production is to remain technically robust and economically viable.

In practice, effective phosphorus control requires a shift in process philosophy: from maximizing TiO_2 content to engineering feedstocks that consistently produce fully rutilized, pigment-grade TiO_2. This shift is essential to reduce operational risk, prevent off-spec production, and ensure the long-term sustainability of titanium pigment manufacturing.

Highlights

1. Phosphorus is a critical impurity governing calcination behavior and TiO_2 pigment viability.
2. Residual P_2O_5 suppresses anatase-to-rutile transformation, yielding non-commercial mixed-phase pigments.
3. Physical, hydrometallurgical, and pyrometallurgical dephosphorization routes are critically compared beyond removal efficiency.
4. Robust phosphorus control requires integrated, feedstock-specific strategies optimized for rutilization performance.

Declarations

Declaration of Competing Interest

The author declares that there are no known competing financial interests or personal relationships that could have influenced the work reported in this paper.

Funding

This research did not receive any specific grant from funding agencies in the public, commercial, or not-for-profit sectors.

Data Availability Statement

No new data were created or analyzed in this study. Data sharing is not applicable to this article.

Author Contributions

The author was responsible for conceptualization, literature review, critical analysis, and manuscript writing.

References

1. Ahn HH, Lee MS. Solvent extraction of Ti(IV) from hydrochloric acid leaching solution of ilmenite. Miner Process Extr Metall Rev. 2021;42(5):312-320. doi:10.1080/08827508.2020.1783713
2. Alfonso P, Hamid SA, Anticoi H, Garcia-Valles M, Oliva J, Tomasa O, *et al*. Liberation characteristics of Ta–Sn ores from Penouta, NW Spain. Minerals. 2020;10(6):509. doi:10.3390/min10060509
3. Álvarez-Manzaneda I, Castaño-Hidalgo Á, de Vicente I. Selecting the most sustainable phosphorus adsorbent for lake restoration: effects on the photosynthetic activity of Chlorella sp. Sustainability. 2024;16(19):8305. doi:10.3390/su16198305
4. Anggraeni VMP, Supriyatna YI, Astuti W, Sumardi S, Prasetya A, Petrus HTBM, *et al*. Ilmenite sand direct leaching kinetics in hydrochloric acid solution. J Sustain Metall. 2023;9(4):1578-1588. doi:10.1007/s40831-023-00687-4
5. Azamat Y, Almagul U, Nina L, Zaure K, Kaysar K. Study of the alkaline treatment effect on separation of silica from the electric melting dust of ilmenite concentrates. Int Multidiscip Sci Geoconf SGEM. 2021;21(1.1):391-399. doi:10.5593/sgem2021/1.1/s04.049
6. Chen W, Liu B, Ding J, Yuwen C, Gong S, Ji G, *et al*. Mechanism and kinetics study on sulfuric acid leaching of titanium from NaOH roasting ilmenite. JOM. 2024;76(9):5365-5375.
7. Daba K, Ramakokovhu MM, Mojisola T, Shongwe MB, Ntholeng N. Iron extraction from South African ilmenite concentrate leaching by hydrochloric acid (HCl) in the presence of reductant (metallic Fe) and additive ($MgSO_4$). Minerals. 2022;12(10):1336. doi:10.3390/min12101336
8. De Oliveira ALB, da Silva GDS, de Aguiar PF, Neumann R, Neto AA, Carneiro MC, *et al*. Optimization of alkaline roasting to enable acid leaching of titanium from anatase ores. J Sustain Metall. 2023;9(1):183-193. doi:10.1007/s40831-022-00572-6
9. Dubenko AV, Nikolenko MV, Kostyniuk A, Likozar B. Sulfuric acid leaching of altered ilmenite using thermal, mechanical and chemical activation. Minerals. 2020;10(6):538. doi:10.3390/min10060538
10. Fang S, Xu L, Wu H, Xu Y, Wang Z, Shu K, *et al*. Influence of surface dissolution on sodium oleate adsorption on ilmenite and its gangue minerals by

ultrasonic treatment. Appl Surf Sci. 2020;500:144038. doi:10.1016/j.apsusc.2019.144038
11. Fouda IM, El-Kady MY, El-Sheikh EM, Orabi AH, Youssef AO. Elimination of Cr(VI), Pb(II), V(V), and Cd(II) ions from titanium oxide pigment from Rosetta ilmenite concentrate using synthesised cellulose phosphorus oxychloride. Int J Environ Anal Chem. 2023;103(17):5795-5814. doi:10.1080/03067319.2022.2031981
12. Georgievskiy AF, Bugina VM. Phosphorites and glauconites as additional reserves in the development of titanium–zirconium sands of the Centralnoye deposit (Tambov region of Russia). IOP Conf Ser Earth Environ Sci. 2022;988(2):022031. doi:10.1088/1755-1315/988/2/022031
13. Gerasimova LG, Maslova MV, Shchukina ES. Synthesis of sorption materials from low-grade titanium raw materials. Materials (Basel). 2022;15(5):1922. doi:10.3390/ma15051922
14. Hildor F, Zevenhoven M, Brink A, Hupa L, Leion H. Understanding the interaction of potassium salts with an ilmenite oxygen carrier under dry and wet conditions. ACS Omega. 2020;5(36):22966-22977. doi:10.1021/acsomega.0c03007
15. Hu C, Yang X, Wang X, Guo P, Li D, Zhu X, *et al*. Impacts of agro-biomass ash on ilmenite oxygen carrier performance in chemical looping combustion: catalytic enhancement and microstructural evolution. Chem Eng Sci. 2025:122755. doi:10.1016/j.ces.2025.122755
16. Hu Q, Yu M, Bi D, Liu J, Huang M, Zhu A, *et al*. Grain size analyses and mineral compositions of core sediments in the western North Pacific Ocean: implications for the rare earth element and yttrium enrichment and deposition environment. Minerals. 2023;13(12):1470. doi:10.3390/min13121470
17. Kepezhinskas P, Berdnikov N, Krutikova V, Kozhemyako N. Iron–titanium oxide–apatite–sulfide–sulfate microinclusions in gabbro and adakite from the Russian Far East indicate possible magmatic links to iron oxide–apatite and iron oxide–copper–gold deposits. Minerals. 2024;14(2):188. doi:10.3390/min14020188
18. Kepezhinskas PK, Berdnikov NV, Krutikova VO, Kozhemiako NV. Assemblages of microinclusions of Fe–Ti oxides, apatite, sulfates, and sulfides in pyroxenites, gabbroids, and adakitic granitoids from the Gabbrovy massif as precursors of IOCG and IOA mineralization. Russ J Pac Geol. 2024;18(6):621-636. doi:10.1134/S1819714024060046
19. Khedr MZ, Moftah A, El-Shibiny NH, Tamura A, Tan W, Ichiyama Y, *et al*. Mineralogy and geochemistry of titaniferous iron ores in El-Baroud layered gabbros: Fe–Ti ore genesis and tectono-metallogenetic setting. Minerals. 2024;14(7):679. doi:10.3390/min14070679
20. Kong X, Bai R, Wang S, Wu B, Zhang R, Li H. Recovery of phosphorus from aqueous solution by magnetic TiO_2/Fe_3O_4 composites. Chem Phys Lett. 2022;787:139234. doi:10.1016/j.cplett.2021.139234
21. Kordzadeh-Kermani V, Schaffie M, Rafsanjani HH, Ranjbar M. A modified process for leaching of ilmenite and production of TiO_2 nanoparticles. Hydrometallurgy. 2020;198:105507. doi:10.1016/j.hydromet.2020.105507
22. Kumari H, Khati P, Gangola S, Chaudhary P, Sharma A. Performance of plant growth promotory rhizobacteria on maize and soil characteristics under the influence of TiO_2 nanoparticles.
23. Li S, Nemchin A, Che X, Liu D, Long T, Luo Y, *et al*. Multiple thermal events recorded in IIE silicate inclusions: evidence from in situ U–Pb dating of phosphates in Weekeroo Station. Geochim Cosmochim Acta. 2021;309:79-95. doi:10.1016/j.gca.2021.06.009
24. Li Z, Xie Z, He D, Deng J, Zhao H, Li H. Simultaneous leaching of rare earth elements and phosphorus from a Chinese phosphate ore using H_3PO_4. Green Process Synth. 2021;10(1):258-267. doi:10.1515/gps-2021-0025
25. Lin Q, Zhang K, McGowan S, Capo E, Shen J. Synergistic impacts of nutrient enrichment and climate change on long-term water quality and ecological dynamics in contrasting shallow-lake zones. Limnol Oceanogr. 2021;66(9):3271-3286. doi:10.1002/lno.11871
26. Long T, Xiang L, Tian C, Liu J, Xiang W, Li L, *et al*. The effect of sulfuric acid concentration on titanium leaching from an ilmenite ore. Results Eng. 2025:108139. doi:10.1016/j.rineng.2024.108139
27. Luo L, Wu H, Yang J, Tang Z, Shu K, Xu Y, *et al*. Effects of microwave pre-treatment on the flotation of ilmenite and titanaugite. Miner Eng. 2020;155:106452. doi:10.1016/j.mineng.2020.106452
28. Lv Y, Le QT, Bui HB, Bui XN, Nguyen H, Nguyen-Thoi T, *et al*. A comparative study of different machine learning algorithms in predicting the content of ilmenite in titanium placer. Appl Sci (Basel). 2020;10(2):635. doi:10.3390/app10020635
29. Luyckx L, Van Caneghem J. Recovery of phosphorus from sewage sludge ash: influence of chemical addition prior to incineration on ash mineralogy and related phosphorus and heavy metal extraction. J Environ Chem Eng. 2022;10(4):108117. doi:10.1016/j.jece.2022.108117
30. Makeyev AB, Borisovsky SE, Krasotkina AO. The chemical composition and age of monazite and kularite from titanium ore of Pizhemskoye and Yarega deposits (Middle and Southern Timan). Georesursy. 2020;22(1):22-31. doi:10.18599/grs.2020.1.22-31
31. Mandende H, Mothupi T. Apatite-rich zones in the Uppermost Upper Zone, Northern Limb, Bushveld Complex: possible non-conventional source of REE and TiO_2. J Geochem Explor. 2024;263:107498. doi:10.1016/j.gexplo.2024.107498
32. Mandende H, Mothupi T. Quantitative mineralogical characterization of the Upper Apatite-Rich Zone of the Bushveld Complex using QEMSCAN®: implications for mineral processing of apatite, ilmenite, and titanomagnetite ore minerals. Ore Energy Resour Geol. 2025:100120. doi:10.1016/j.oregeorev.2025.100120
33. Mao S, Zhang Q. Mineralogical characteristics of phosphate tailings for comprehensive utilization. Adv Civ Eng. 2021;2021:5529021. doi:10.1155/2021/5529021
34. Miloski P, Dare S, Morisset CE, Davies JH, Perrot MG, Savard D. Petrogenesis of Fe–Ti–P mineral deposits associated with Proterozoic anorthosite massifs in the Grenville Province: insights from oxide and apatite trace-element geochemistry at Lac à l'Orignal, Quebec, Canada. Miner Depos. 2024;59(3):519-556. doi:10.1007/s00126-023-01213-7
35. Mogahed MM. Tracing magmatic physicochemical conditions in Abu Kharief alkali granite, North-Eastern

Desert, Egypt: evidences from apatite, magnetite & ilmenite chemistry. Arab J Geosci. 2020;13:1185. doi:10.1007/s12517-020-06130-4
36. Mogashane TM, Moswane R, Mapazi O, Motlatle MA, Mashale K, Mokoena L, *et al*. Comparison and optimization of analytical techniques for accurate phosphorus determination in high-titanium geological samples. Environ Technol Innov. 2025:104384. doi:10.1016/j.eti.2025.104384
37. Nabil H, Barnes SJ. Origin of the apatite–ilmenite deposit of Sept-Îles, Québec, Canada. In: Mineral deposits at the beginning of the 21st century. Boca Raton: CRC Press; 2022. p. 611-614. doi:10.1201/9781003321552-155
38. Nshimiyimana P, Fagel N, Messan A, Wetshondo DO, Courard L. Physico-chemical and mineralogical characterization of clay materials suitable for production of stabilized compressed earth blocks. Constr Build Mater. 2020;241:118097. doi:10.1016/j.conbuildmat.2020.118097
39. Page MJ, McKenzie JE, Bossuyt PM, Boutron I, Hoffmann TC, Mulrow CD, *et al*. The PRISMA 2020 statement: an updated guideline for reporting systematic reviews. BMJ. 2021;372:n71. doi:10.1136/bmj.n71
40. Pincus LN, Petrović PV, Gonzalez IS, Stavitski E, Fishman ZS, Rudel HE, *et al*. Selective adsorption of arsenic over phosphate by transition metal cross-linked chitosan. Chem Eng J. 2021;412:128582. doi:10.1016/j.cej.2021.128582
41. Pysarenko S, Kaminskyi O, Chyhyrynets O, Denysiuk R, Anichkina O, Chernenko V. Kinetics of alkaline leaching process of titanium (IV) from ilmenite. J Chem Technol Metall. 2023;58(6):1146-1152.
42. Qu Y, Xing L, Gao M, Zhao S, Ren Q, Li L, *et al*. Progress and prospects for titanium extraction from titanium-bearing blast furnace slag. Materials (Basel). 2024;17(24):6291. doi:10.3390/ma17246291
43. Rampfumedzi T, Mkhohlakali A, Cingo X, Mogashane T, Letsoalo MR, Mokgosi D, *et al*. Dissolution and characterization techniques of high-value base metals from various mineral ore matrices: realization for energy application.
44. Reich M, Simon AC, Barra F, Palma G, Hou T, Bilenker LD. Formation of iron oxide–apatite deposits. Nat Rev Earth Environ. 2022;3(11):758-775. doi:10.1038/s43017-022-00313-3
45. Rodriguez-Mustafa MA, Simon AC, del Real I, Thompson JF, Bilenker LD, Barra F, *et al*. A continuum from iron oxide copper–gold to iron oxide–apatite deposits: evidence from Fe and O stable isotopes and trace element chemistry of magnetite. Econ Geol. 2020;115(7):1443-1459. doi:10.5382/econgeo.4739
46. Rotich NK, Herdzik-Koniecko I, Smolinski T, Kalbarczyk P, Sudlitz M, Rogowski M, *et al*. Recovery of metals from titanium ore using solvent extraction process: part 1—transition metals. Minerals. 2024;14(12):1212. doi:10.3390/min14121212
47. Shuai Q, Xu Z, Yao Z, Chen X, Jiang Z, Peng X, *et al*. Fire resistance of phosphoric acid-based geopolymer foams fabricated from metakaolin and hydrogen peroxide. Mater Lett. 2020;263:127228. doi:10.1016/j.matlet.2019.127228
48. Spencer W, Ibana D, Singh P, Nikoloski AN. Effect of borax-, KOH-, and NaOH-treated coal on reducing carbon waste and activated carbon production in synthetic rutile production from ilmenite. Clean Technol. 2025;7(4):92. doi:10.3390/cleantech7040092
49. Stopic S, Kostić D, Emil-Kaya E, Uysal E, Gürmen S, Mitrašinović A, *et al*. High-pressure and high-temperature dissolution of titanium from titanium and aluminum residues: a comparative study. Surfaces. 2024;7(4):1096-1108. doi:10.3390/surfaces7040070
50. Su JH, Zhao XF, Li XC, Su ZK, Liu R, Qin ZJ, *et al*. Fingerprinting REE mineralization and hydrothermal remobilization history of the carbonatite–alkaline complexes, Central China: constraints from in situ elemental and isotopic analyses of phosphate minerals. Am Mineral. 2021;106(10):1545-1558. doi:10.2138/am-2021-7742
51. Subasinghe HCS, Ratnayake AS. Mechanical activation and physicochemical factors controlling pyrometallurgical, hydrometallurgical, and electrometallurgical processing of titanium ore: a review. J South Afr Inst Min Metall. 2023;123(8):399-414. doi:10.17159/2411-9717/2023/v123n8a2
52. Supriyatna YI, Astuti W, Sumardi S, Prasetya A, Petrus HTBM, Dida EN. Kinetics study of low-grade ilmenite fusion process using sodium hydroxide: non-isothermal condition with model-free methods. Mater Today Proc. 2023. doi:10.1016/j.matpr.2023.02.391
53. Tahooni Bonab S, Abdollahi H, Abbaspour A. The hydrometallurgical approach in the production of a high content of titanium dioxide (TiO_2) from ilmenite: direct hydrochloric and sulfuric acid leaching and pre-treatment methods—a review. Miner Process Extr Metall Rev. 2025;46(4):537-553. doi:10.1080/08827508.2024.2320906
54. Thambiliyagodage C, Wijesekera R, Bakker MG. Leaching of ilmenite to produce titanium-based materials: a review. Discov Mater. 2021;1(1):20. doi:10.1007/s43939-021-00020-4
55. Tonello MS, Hebner TS, Sterner RW, Brovold S, Tiecher T, Bortoluzzi EC, *et al*. Geochemistry and mineralogy of southwestern Lake Superior sediments with an emphasis on phosphorus lability. J Soils Sediments. 2020;20(2):1060-1073. doi:10.1007/s11368-019-02467-5
56. Üçerler-Çamur Z, Keleş O, Kangal MO. Mineral liberation analysis (MLA)-based characterization of lithium source: biotite and associated minerals in nepheline syenites. Minerals. 2025;15(8):876. doi:10.3390/min15080876
57. Wang J, Jiang T. Comparative study on grinding kinetics behavior of vanadium–titanium magnetite ore before and after microwave pretreatment. Metall Res Technol. 2024;121(2):211. doi:10.1051/metal/2024023
58. Wang K, He H, Shi W. Geochemistry and mineralogy of ilmenite exsolutions in titanomagnetite and their implications for the ore-forming process at the Damiao deposit. Acta Geochim. 2025:1-17. doi:10.1007/s11631-025-00621-3
59. Wulan HE, Zakkiya HN, Sari NA, Ibrahim I. Understanding mineral liberation for copper-sulfide ore mineralogy characterization using automated mineral liberation analysis (MLA).
60. Xiang L, Long T, Liu JS, Xiang WR, Li L, Zhang XR, *et al*. Ultrasound-enhanced ilmenite acid leaching and optimization research. Physicochem Probl Miner

Process. 2025;61(4).
61. Xiao J, Chen C, Ding W, Peng Y, Chen T, Zou K. Extraction of phosphorus from a phosphorus-containing vanadium titano-magnetite tailing by direct flotation. Processes (Basel). 2020;8(7):874. doi:10.3390/pr8070874
62. Xu G, Wang P. Study on the mineral characteristics and upgrading of titanium iron ore concentrate in the Panxi region of China. E3S Web Conf. 2025;617:01017. doi:10.1051/e3sconf/202561701017
63. Yang J, Zhu P, Ma S. Application of MLA in analysis of limonite bearing-zinc ore. J Phys Conf Ser. 2021;2044(1):012097. doi:10.1088/1742-6596/2044/1/012097
64. Yan P, Zhang Y, Zheng S. Microscale spherical TiO_2 powder prepared by hydrolysis of $TiCl_4$ solution: synthesis and kinetics. Particuology. 2024;84:60-71. doi:10.1016/j.partic.2023.05.008
65. Yoo S, Chae J, Oh JM, Lim JW. Effect of ultrasonic cleaning of titanium turning scraps immersed in alkaline solution and subsequent preparation of ferrotitanium ingots. Korean J Met Mater. 2021;59(2):113-120. doi:10.3365/KJMM.2021.59.2.113
66. Zeng LP, Zhao XF, Spandler C, Hu H, Hu B, Li JW, *et al*. Origin of high-Ti magnetite in magmatic–hydrothermal systems: evidence from iron oxide–apatite (IOA) deposits of eastern China. Econ Geol. 2022;117(4):923-942. doi:10.5382/econgeo.4917
67. Zhai J, Chen P, Sun W, Chen W, Wan S. A review of mineral processing of ilmenite by flotation. Miner Eng. 2020;157:106558. doi:10.1016/j.mineng.2020.106558
68. Zhang B, Wang R, Liu C, Jiang M. Self-digestion of Cr-bearing vanadium slag processing residue via hot metal pre-treatment in steelmaking process. Metall Mater Trans B. 2022;53(2):1183-1195. doi:10.1007/s11663-021-02452-3
69. Zhang H, Sun W, Zhang C, He J, Chen D, Zhu Y. Adsorption performance and mechanism of the commonly used collectors with oxygen-containing functional group on the ilmenite surface: a DFT study. J Mol Liq. 2022;346:117829. doi:10.1016/j.molliq.2021.117829
70. Zhang J, Dong Y, Li Y, Yang L, Jia X, Zhang L, *et al*. The effect of phosphate/TiO_2 composite insulating layer on the high-frequency magnetic properties of FeSiBPCNbCu nanocrystalline soft magnetic powder cores. Mater Today Commun. 2024;38:107809. doi:10.1016/j.mtcomm.2023.107809
71. Zhang Y, Fang ZZ, Sun P, Huang Z, Zheng S. A study on the synthesis of coarse TiO_2 powder with controlled particle sizes and morphology via hydrolysis. Powder Technol. 2021;393:650-658. doi:10.1016/j.powtec.2021.07.048
72. Zhukova IA, Stepanov AS, Korsakov AV, Jiang SY. Application of Raman spectroscopy for the identification of phosphate minerals from REE supergene deposit. J Raman Spectrosc. 2022;53(3):485-496. doi:10.1002/jrs.6291

How to Cite This Article
Pereira AC. Phosphorus control in titanium feedstocks for TiO_2 pigment production: A critical review of mineralogical constraints, dephosphorization routes, and rutilization performance. International Journal of Future Engineering Innovations. 2026;3(2):8-30. doi:10.54660/IJFEI.2026.3.2.08-30.